High Temperature PEM Fuel Cells - Degradation and Durability

Araya, Samuel Simon

Publication date:
2012

Document Version
Publisher's PDF, also known as Version of record

AALBORG UNIVERSITET

HIGH TEMPERATURE PEM FUEL CELLS

Degradation & Durability

Samuel Simon Araya

Department of
ENERGY TECHNOLOGY
E.T.

High Temperature PEM Fuel Cells Degradation & Durability

Samuel Simon Araya

Dissertation submitted to the Faculty of Engineering and Science
at Aalborg University in partial fulfillment of the
requirements for the degree of

DOCTOR OF PHILOSOPHY

Aalborg University
Department of Energy Technology
Aalborg, Denmark
December 2012

High Temperature PEM Fuel Cells – Degradation & Durability

ISBN 978-87-92846-14-3

Printed in Denmark by UniPrint

Aalborg University
Department of Energy Technology
Pontoppidanstraede 101
9220 Aalborg Øst
Denmark

To my family

Abstract

Samuel Simon Araya
December – 2012

A harmonious mix of renewable and alternative energy sources, including fuel cells is necessary to mitigate problems associated with the current fossil fuel based energy system, like air pollution, Greenhouse Gas (GHG) emissions, and economic dependence on oil, and therefore on unstable areas of the globe. Fuel cells can harness the excess energy from other renewable sources, such as the big players in the renewable energy market, Photovoltaic (PV) panels and wind turbines, which inherently suffer from intermittency problems. The excess energy can be used to produce hydrogen from water or can be stored in liquid alcohols such as methanol, which can be sources of hydrogen for fuel cell applications. In addition, fuel cells unlike other technologies can use a variety of other fuels that can provide a source of hydrogen, such as biogas, methane, butane, etc. More fuel flexibility combined with wider range of applications than any other available technology make them suitable candidates for powering a sustainable future.

This work analyses the degradation issues of a High Temperature Proton Exchange Memebrane Fuel Cell (HT-PEMFC). It is based on the assumption that given the current challenges for storage and distribution of hydrogen, it is more practical to use liquid alcohols as energy carriers for fuel cells. Among these, methanol is very attractive, as it can be obtained from a variety of renewable sources and has a relatively low reforming temperature for the production of hydrogen rich gaseous mixture. The effects on HT-PEMFC of the different constituents of this gaseous mixture, known as a reformate gas, are investigated in the current work. For this, an experimental set up, in which all these constituents can be fed to the anode side of a fuel cell for testing, is put in place. It includes mass flow controllers for the gaseous species, and a vapor delivery system for the vapor mixture of the unconverted reforming reactants.

Electrochemical Impedance Spectroscopy (EIS) is used to characterize the effects of these impurities. The effects of CO were tested up to 2% by volume along with other impurities. All the reformate impurities, including methanol-water vapor mixture, cause loss in the performance of the fuel cell. In general, CO_2 dilutes

the reactants, if tested alone at high operating temperatures ($\sim$180 °C), but tends to exacerbate the effects of CO if they are tested together. On the other hand, CO and methanol-water vapor mixture degrade the fuel cell proportionally to the amounts in which they are tested. In this dissertation some of the mechanisms with which the impurities affect the fuel cell are discussed and interdependence among the effects is also studied. This showed that the combined effect of reformate impurities is more than the arithmetic sum of the individual effects of reformate constituents.

The results of the thesis help to understand better the issues of degradation and durability in fuel cells, which can help to make them more durable and competitive with traditional devices to revolutionize the current energy systems.

Dansk Resumé

En større udbredelse af vedvarende og alternative energikilder, herunder brændselsceller er nødvendigt for at mindske problemerne i forbindelse med det nuværende fossile brændstof baseret energisystem. Problemer som luftforurening, drivhusgasemissioner, og økonomisk afhængighed af råolie, der hovedsageligt forekommer i ustabile områder i verden, har fundet sted i mange år, og de bestråbelser og tilsagn, der træffes af nationale og internationale organer har kun forsinket processen lidt, men har ikke løst problemerne.

Afhandlingen beskriver degraderingsmekanismerne i brændselsceller. Brændselsceller er elektro-kemiske enheder der laver elektricitet ved direkte kemisk omdannelse af gasformige brændsler, så som hydrogen og andre hydrogen-rige blandinger. Brændselsceller har vist sig at have en række fordele frem for traditionelle teknologier, bl.a. højere virkningsgrader, bedre brændstof fleksibilitet, samt miljømæssige og samfundsøkonomiske fordele. Brændselsceller kan udnytte den overskydende energi fra andre vedvarende energikilder, som f.eks. solcellepaneler og vindmøller. De kan være en løsning på udfordringen med vindkraftens diskontinuitet. Den overskydende energi kan anvendes til fremstilling af brint fra vand, som kan lagres i flydende alkoholer, f.eks. methanol, der kan være brintbære til brug i brændselsceller. Desuden kan brændselsceller i modsætning til andre teknologier anvende en række andre brændsler, der kan fungere som brintbære, f.eks. biogas, methan, butan osv. Højere brændstof fleksibilitet kombineret med et bredere anvendelsesområde end nogen anden tilgængelig teknologi gør dem egnede kandidater til at drive en bæredygtig fremtid.

Løsninger i forhold til pris og pålidelighed skal dog stadig findes før deres endelige kommercialisering og indtræden i hverdagen bliver mulig. Dette forskningsprojekt er initieret for at adressere problemstillingerne omkring holdbarhed og for at analysere forskellige degraderingsmekanismer for en særlig type brændselscelle, kendt som High Temperature Proton Exchange Membrane Fuel Cell (HT-PEMFC). Projektet beskriver de primære fejltilstande og stressfaktorer.

På grund af de aktuelle udfordringer for produktion og distribution af brint, er det mere praktisk at bruge flydende alkoholer som energibærere til brændselsceller. Blandt disse er methanol meget attraktiv, da det kan produceres fra en række af vedvarende energikilder og har en relativt lav dampreformerings temperatur til fremstilling af hydrogen-rige blandinger. Det aktuelle arbejde undersøger virkningerne på en HT-PEMFC af de forskellige bestanddele af disse hydrogen-rige blandinger. Til dette blev en eksperimentel opstilling forberedt,

hvor alle enkeltdelene kan tilføres anodesiden af en brændselscelle. Opstillingen omfatter massestrømskontrollere til de gasformige arter og en fordamper til de uomdannede reaktanter.

I dette arbejde er elektrokemisk impedansspektroskopi (EIS) brugt til at karakterisere virkningerne af disse urenheder. Virkningerne af CO er undersøgt op til 2 volume % sammen med andre urenheder. Alle reformerings urenheder, herunder dampblanding af methanol og vand, medfører et tab i brændselscellen. Virkningen af CO_2 er kun en fortynding af reaktanterne, når det testes alene ved høje arbejdstemperaturer ($\sim$180 °C), men har en tendens til at forstørre virkningerne af CO . Påden anden side nedbryder CO og en dampblanding af methanol og vand brændselscellen afhængigt af, hvor meget der findes i gasblandingen. I denne afhandling er nogle af de mekanismer, som urenhederne påvirker brændselscellen med, diskuteret og den indbyrdes afhængighed mellem deres bidrag er også undersøgt. Det viser sig, at de kombinerede virkninger af dampreformerings urenheder er større end den aritmetiske sum af den individuelle virkning af bestanddelene.

Resultaterne af afhandlingen bidrager til en bedre forståelse af degradering og udholdenhed af brændselsceller, hvilket kan have betydning for arbejdet med at gøre dem mere holdbare og konkurrencedygtige i forhold til mere traditionelle teknologier, og dermed revolutionere det nuværende energi system. Brændselsceller kan fremstilles i forskellige størrelser og til forskellige applikationer, heriblandt, el og varme til husholdninger, samt el og varme til mobile applikationer.

Eksperimenterne i forbindelse med afhandlingen blev udført I brændselscelle laboratoriet på Insitut for Energiteknik, Aalborg Universitet i samarbejde med Serenergy A/S. Resultaterne er formidlet internationalt i form af konferencer og videnskabelige tidsskrifter.

Acknowledgements

Free at last ⌣̈, just a sigh of relief. Undertaking a PhD fellowship, with all its ups and downs, has been one of the most rewarding and exciting experiences I've ever had. Obviously, it could not have been so without the help and the guidance of many whom I'm deeply indebted to.

First and foremost, I would like to express my deepest gratitude to Professor Søren Knudsen Kær, my research supervisor, for his patient guidance, encouragement and useful critiques of this research work. I am also heartily thankful to my co–supervisor Professor Søren Juhl Andreasen for his assistance at all the stages of the project, in preparing the experimental setup, setting the LabView control program, and afterwards discussing experimental results.

At the same time, I'm very grateful to my colleagues Jakob Rabjerg Vang, Vincezo Liso, Benoît Bidoggia and Haftor Örn Sigurdsson for reviewing and discussing my work from time to time and giving me valuable feedback, and to Simon Lennart Sahlin for his assistance in the laboratory. The same gratitude goes to all my colleagues for their support in many ways to my project and for the great working environment they provide.

I would like to extend my gratitude to the technicians of the fuel cell laboratory at our department for their patient assistance in preparing and modifying the experimental setup several times.

I'm indebted to my parents, and all my siblings for their understanding, support and encouragement throughout the years of my stay far from home.

People are what constitute a good community and I would like to recognize that in all the people that I've met in the city of Aalborg, and the great friends that I've made throughout my time here. Without my friends, undertaking such a long engagement would not have been possible, and therefore, my most sincere thanks go to all of them.

Lastly, I offer my regards and blessings to all of those who supported me in any respect during the completion of the project.

Aalborg, December 2012 *Samuel Simon Araya*

Thesis Outline

Guide to the Reader

This dissertation is prepared as a collection of scientific papers produced during the PhD period, and relevant to the project based on the objectives set at the beginning of the research work. Accordingly the main body of the thesis is made up of 5 chapters, which are divided as follows;

Chapter 1 describes the current energy system in relation to fuel cells and states the motivation for the current research work. It describes the fuel cell generalities and gives an overview of the role of fuel cells in the future of energy systems.

Chapter 2 gives a background on the type of fuel cell under investigation in this research project, an HT-PEMFC. After describing the working principles, it presents the different components that make up an HT-PEMFC. It then highlights the main degradation modes and characterization methods as part of the literature review for the project.

Chapter 3 is where the methodology for the work, fuel cell test station is described. The chapter is a summary of the work published in *paper 1* on a dedicated vapor delivery system, prepared for the purpose of studying the effects of methanol–water vapor mixture. Lastly some of the condition for the tests and techniques used to analyze the EIS data acquired in the tests are explained.

Chapter 4 summarizes the main contributions of the current research project in relation to the available literature and the objectives of the project. For easy reading the chapter is divided in to sections that analyze the effects of impurities separately, and therefore, results from the different tests are put together for an overall analysis. The combined effects of impurities were also qualitatively compared with individual effects of the impurities.

Chapter 5 Concludes the dissertation by giving the final remarks and addressing the limitations of the work for possible improvements for future work in experimental characterization of HT-PEMFCs.

The experimental work in this thesis is entirely undertaken in the fuel cell laboratory at the department of energy technology, Aalborg University in collaboration

with Serenergy A/S. The test station is prepared together with the help of my supervisors Søren Knudsen Kær and Søren Juhl Andreasen.

In this dissertation the acronyms PEMFC and LT-PEMFC are used interchangeably, and they both refer to proton exchange membrane fuel cells that employ Nafion®–based polymer membrane for operation at temperatures below 100 °C.

List of Publications

The following is a list of publications and other means of dissemination produced during my PhD fellowship at the Department of Energy Technology, Aalborg University, Denmark.

Journal papers

Paper 1 Vapor Delivery Systems for the Study of the Effects of Reformate Gas Impurities in HT-PEM Fuel Cells
Simon Araya, Samuel; Kær, Søren Knudsen; Andreasen, Søren Juhl.
Published in *Journal of Fuel Cell Science and Technology*. 2012.

Paper 2 Experimental Characterization of the Poisoning Effects of Methanol–Based Reformate Impurities on a PBI–Based High Temperature PEM Fuel Cell
Simon Araya, Samuel; Andreasen, Søren Juhl; Kær, Søren Knudsen.
Published in *Energies in special issue: Hydrogen Energy and Fuel Cells*. 2012.

Paper 3 Investigating the Effects of Methanol-Water Vapor Mixture on a PBI–Based High Temperature PEM Fuel Cell
Simon Araya, Samuel; Andreasen, Søren Juhl; Nielsen, Heidi Venstrup; Kær, Søren Knudsen.
Published in *International Journal of Hydrogen Energy*. 2012.

Conference papers and presentations

Paper 4 EIS Characterization of the Poisoning Effects of CO and CO_2 on a PBI Based HT-PEM Fuel Cell
Andreasen, Søren Juhl; Mosbæk, Rasmus; Vang, Jakob Rabjerg; Kær, Søren Knudsen; **Simon Araya, Samuel**.
Published in *ASME Conference Proceedings*, 2010;(44045):27–36.

Paper 5 Analysis of the Effects of Methanol, CO, CO_2 and Water Vapor in a CH_3PO_4/PBI–based HT-PEMFC by Means of EIS
Simon Araya, Samuel; Andreasen, Søren Juhl; Kær, Søren Knudsen.
Presented in *ASME 2011 5th International Conference on Energy Sustainability & 9th Fuel Cell Science, Engineering and Technology Conference*, August, 2011. Abstract. Oral presentation.

Contents

List of Figures

List of Tables

Abbreviations

Acronyms	
AC	Alternating Current
APU	Auxiliary Power Unit
AST	Accelerated Stress Test
CL	Catalyst Layer
CNLS	Complex Non-linear Least-Square
CV	Cyclic Voltametry
DC	Direct Current
DEFC	Direct Ethanol Fuel Cell
DMFC	Direct Methanol Fuel Cell
DOE	U.S. Department of Energy
EC	Equivalent Circuit
ECSA	Electrochemical Surface Area
EDS	Energy-Dispersive X-ray Spectroscopy
EIS	Electrochemical Impedance Spectroscopy
FCEV	Fuel Cell Electric Vehicle
FCH–JU	Fuel Cells and Hydrogen Join Undertaking
FTIR	Fourier Transform InfraRed
GC	Gas Chromatography
GDL	Gas Diffusion Layer
GHG	Greenhouse Gas
HT-PEMFC	High Temperature Proton Exchange Membrane Fuel Cell
ICE	Internal Combustion Engine
IEA	International Energy Agency
JHFC	Japan Hydrogen & Fuel Cell Demonstration Project
LT-PEMFC	Low Temperature Proton Exchange Membrane Fuel Cell
MCFC	Molten Carbonate Fuel Cell
MEA	Membrane Electrode Assembly
MPL	Mirco-Porous Layer
MS	Mass Spectroscopy
NASA	National Aeronautics and Space Administration
NMR	Nuclear Magnetic Resonance

Continued on next page

Abbreviations– continued from previous page

Acronyms	
OCV	Open Circuit Voltage
ORR	Oxygen Reduction Reaction
PA	Phosphoric Acid
PAFC	Phosphoric Acid Fuel Cell
PBI	Polybenzimidazole
PEM	Proton Exchange Membrane
PEMFC	Proton Exchange Membrane Fuel Cell
PFSA	Perfluorosulphonic Acid
PROX	Preferential Oxidation
PV	Photovoltaic
REN21	Renewable Energy Policy Network for the 21st Century
RH	Relative Humidity
R_{hf}	High Frequency Resistance
R_{if}	Intermediate Frequency Resistance
R_{lf}	Low Frequency Resistance
R_{ohmic}	Ohmic Resistance
RWGS	Reverse Water Gas Shift
SEM	Scanning Electron Microscopy
SOFC	Solid Oxide Fuel Cell
TEM	Transmission Electron Microscopy
UPS	Uninterrupted Power Supply
WGS	Water Gas Shift

1 Introduction

"What's the use of a fine house if you haven't got a tolerable planet to put it on?"

- Henry David Thoreau.

This section gives a brief overview of the current energy system and states the motivation for the current research work. It then describes the fundamentals of fuel cell technology, gives a brief history and outlines research and technology trends.

1.1 Overview

1.1.1 Why Fuel Cells?

With the increasing urgency for action to mitigate climate change and its consequences, several renewable and alternative options for energy generation, conversion and storage are being developed and continuously studied around the globe. Investments on renewable energy are increasing every year despite the extended period of global economic recession, with China being the leading country in total investment in renewable energy for the year 2011 [REN21, 2012]. However, despite all the efforts and pressure by the international bodies for climate change mitigation, the global CO_2 emissions rose by 3.2% in the last year alone compared to 2010, where it hit an all-time high of 31.6 Gt according to preliminary estimates from the International Energy Agency (IEA) [IEA, 2012]. In Fig. 1.1 the global CO_2 emission from the main anthropogenic causes, use of fossil fuel ad cement production is provided by region.

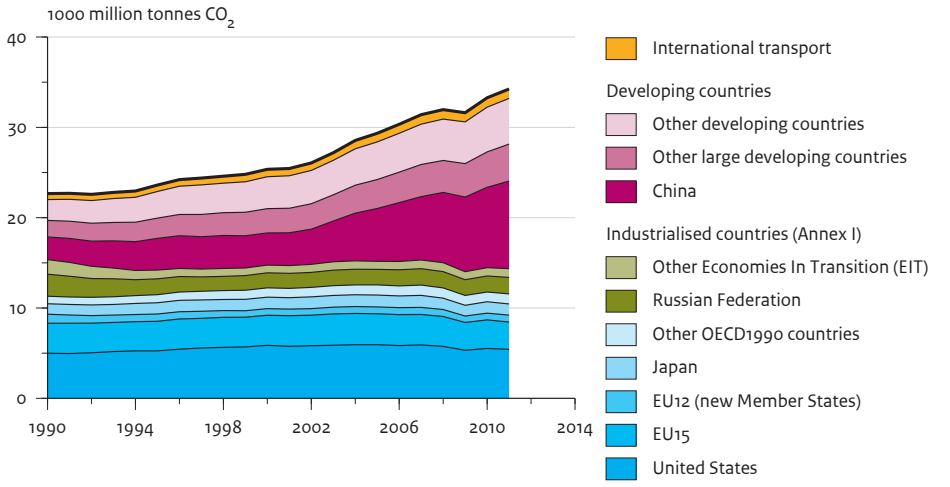

Source: EDGAR 4.2 (1970–2008); IEA, 2011; USGS, 2012; WSA, 2012; NOAA, 2012

Figure 1.1: Global CO_2 emission from fossil fuel use and cement production. *Reproduced from Oliver et al. [2012].*

Therefore, never before has there been so much need for transition from the current energy system, which still rely mainly on fossil fuels to a new and alternative system based on renewable sources. To favor this transition, there are a number of initiatives that are catalyzing the increased market share of green energy, from policy trends to increased investment and national and international goals to decrease fossil based power generation. According to Renewable Energy Policy Network for the 21st Century (REN21) [REN21, 2012] annual report, at least 118 countries, more than half of which are developing countries, had renewable energy targets in place by early 2012. There are concentric targets that go from global to regional, national, provincial and to municipal, which usually tend to be more and more ambitious as the area of interest narrows down to smaller areas. The targets vary from a few percentage increase in renewable energy production in some countries to other ambitious ones such as the 100% renewable energy target reached by Denmark for the year 2050 [Danish Energy Agency, 2009].

For these targets to be met, however, a harmonious mix of renewable sources of various nature for different sectors should be put in place. Fuel cells, being one of the most versatile energy conversion devices are expected to play an important role in achieving these goals and in mitigating some of the major issues associated with current energy sources. Theoretically, they can suitably power mobile phones and cities alike, and when supplied with hydrogen derived from renew-

able energy sources (solar, wind, biomass, etc.), they can can be 100% CO_2 neutral and positively impact the environment. Other advantages of fuel cells include, a generally higher efficiency compared to combustion engines, absence of moving parts, which translates into silent and potentially reliable operation, fuel flexibility, and little or no emissions during operation [Ryan O'Hayre, 2004]. As with all renewable energy sources they also contribute to socio-economic development, energy security and energy independence. These advantages are in line with the policy makers' wish for a sustainable development, with more job creation, currently accounting for close to 5 million jobs [International Labour Organization, 2012] globally in renewable energy industries, and wider energy access, including remote areas.

Therefore, together with other renewable sources, fuel cells can reduce the problems associated with petroleum based energy production, which include air pollution, Greenhouse Gas (GHG) emissions, and economic dependence on oil, and therefore on limited resources and unstable areas of the globe. As the big players in the renewable energy market PV and wind energy suffer from intermittency problems, fuel cells can harness the excess energy that can be used to produce hydrogen from water, or can be stored in the form of liquid alcohols. In addition, fuel cells unlike other technologies can use a variety of fuels that can provide a source of hydrogen, such as methanol, biogas, methane, butane, etc. More fuel flexibility combined with wider range of applications than any other available technology makes them suitable candidates for powering a sustainable future.

1.2 Fuel Cell Fundamentals

A fuel cell is an electrochemical device that converts the internal energy of gases into electrical energy, directly and continuously through chemical reactions. The reactions take place as half-cell reactions on the electrode surfaces. An oxidation half-cell reaction takes place on the negative electrode, *anode* according to Eqn. 1.1, and the reduction half reaction takes place on the positive electrode, *cathode* according to Eqn. 1.2,

$$Anode : \mathrm{H_2} \longleftrightarrow 2\,\mathrm{H^+} + 2\,\mathrm{e^-}, \tag{1.1}$$

$$Cathode : \tfrac{1}{2}\,\mathrm{O_2} + 2\,\mathrm{H^+} + 2\,\mathrm{e^-} \longleftrightarrow \mathrm{H_2O}. \tag{1.2}$$

When a fuel cell is fed with pure hydrogen and oxygen, the only exhaust of the process are excess heat and water vapor, which makes fuel cells one of the cleanest technologies currently available, provided that the H_2 gas is obtained from renewable sources. The schematic in Fig. 1.2 illustrates a simple unit H_2/O_2 - based fuel cell assembly, and gives the basic flows and working principles.

Since the voltage output of a single cells is limited to the range 0.6 - 0.8 V, fuel cells are normally connected in series for real life applications to achieve higher voltages, where the overall voltage is the sum of individual ones in this case. Their modular structure allows them to cover a wide range of applications determined

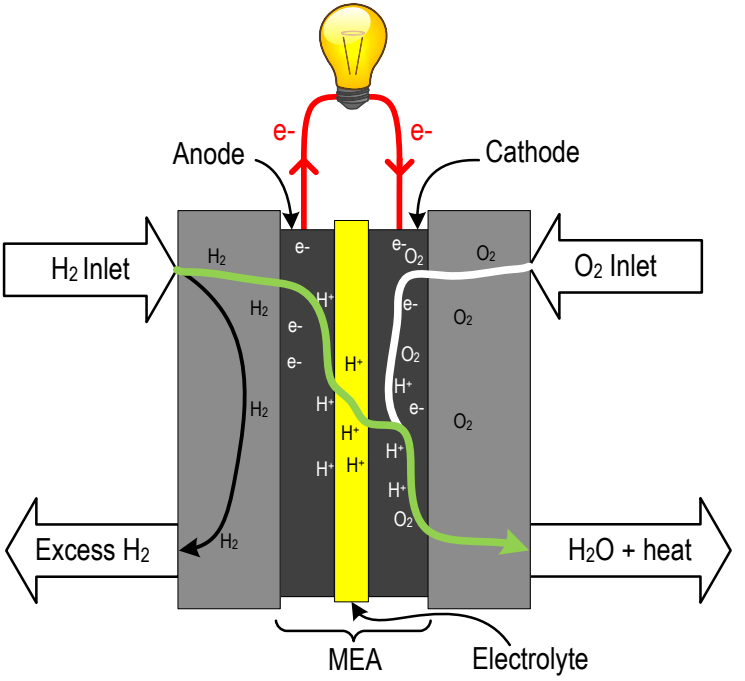

Figure 1.2: Working principle of a fuel cell.

by the type of electrolyte used, the operating temperature and the number of unit cells assembled.

The concept of fuel cells dates back to more than two centuries ago, where Humphry Davy demonstrated the working principle in 1802. Their invention however, is usually attributed to Sir William Grove, a Welsh judge and physical scientist, who invented what he named as *"gas voltaic battery"* in 1839 [University of Cambridge, 2012]. Long after, PEM fuel cells were invented at General Electric in the early 1960s, through the work of Thomas Grubb and Leonard Niedrach, where they later started collaboration with National Aeronautics and Space Administration (NASA) for their use in the Gemini space missions [Smithsonian Institution, 2004]. In the 1970s, due to climate change, oil depletion and energy dependency concerns, fuel cell's as other renewable energy sources started to gain more attention. Since then their development can be said accelerating every decade up until the present time.

1.3 Classification of Fuel Cells

Fuel cells are usually classified based on the electrolyte they employ and sometimes based on the temperature range at which they operate, both factors which determine the suitable application area of a fuel cell. This is one among many advantages of fuel cells with respect to other technologies, where there is a type of fuel cell for almost any application where power is needed. The main types of fuel cells and their properties are summarized in Tab. 1.1.

Table 1.1: Classification of relevant fuel cell types [Fuel Cell Today, 2011]

FC type	Electrolyte	Operating temperature	Electrical efficiency	Typical electrical power	Applications
PEMFC	Ion exchange membrane (water-based)	80 °C	40-60%	< 250 kW	Vehicles, small stationary
HT-PEMFC	Ion exchange membrane (acid-based)	120-200°C	60%	< 100 kW	small staionary
DMFC	Polymer membrane	60-130°C	40%	< 1 kW	Portable
MCFC	Immobilised liquid molten carbonate	650°C	45-60%	> 200 kW	Stationary
PAFC	Immobilised liquid phosphoric acid	200°C	35-40%	> 50 kW	Stationary
SOFC	Ceramic	1000°C	50-65%	< 200 kW	Stationary
AFC	Potassium hydroxide	60-90°C	45-60%	> 20 kW	Submarines, spacecraft

1.4 Technology State of the Art and Trends

There are several national and international, governmental and private funding bodies that are helping the fuel cell development move forward. Projects and goals by U.S. Department of Energy (DOE) and the Fuel Cells and Hydrogen Join Undertaking (FCH–JU) by the European Commission, can be mentioned among others. Japan also made several efforts and commitments with its Ene-farm program, a μ–CHP program for single households and the Japan Hydrogen & Fuel Cell Demonstration Project (JHFC) project, which consists of fuel cell vehicle and hydrogen infrastructure demonstrations. South Korea's investments on the tech-

nology, are also worth mentioning. For-example, POSCO Power completed the construction of its fuel cell stack manufacturing plant in the city of Pohang, South Korea, with current production capacity of 100 MW of Molten Carbonate Fuel Cell (MCFC) stacks annually [Breakthrough Technologies Institute Inc., 2012]

Moreover, there are independent analysts that suggest the commercial success of fuel cells may be imminent. According to an industry review by Fuel Cell Today [2011], fuel cell sales are growing rapidly, around 75% each year since 2007, which is when their commercialization started. The review also says that Proton Exchange Membrane Fuel Cells (PEMFCs) are dominating the early market by selling 97% of total fuel cells sold in 2010, with the most recent review reporting that this grew further by 87.2% in 2011 [Fuel Cell Today, 2012]. A statement from the review summarizes this momentum that fuel cells are currently enjoying and the prospect for their future success as follows,

> "Fuel cells have never been in a better position to positively impact our everyday lives and enjoy the commercial success promised for so long."

As already mentioned and can be noted in Tab. 1.1, the different fuel cell types are appropriate for different areas of application based on their operating temperature and the materials they employ. This means different fuel cell types are suited for different durability targets, operational stresses and power demands. Because of this and variations in research investments they have different development histories, and consequently different achievements and future trends can be foreseen.

1.4.1 Transport Application

The current global transportation system based on petroleum is a huge contributor to the global CO_2 and other GHG emissions, accounting to 23% of the total CO_2 in 2009 [Schipper et al., 2009]. For decades fuels cells have given many promises to free us from the oil bond, especially in regards to automotive applications. However, many years of postponement of their commercialization has resulted in some skepticism and cuts in government funds in some countries. In the US, for example, energy secretary Steven Chu did not trust hydrogen-powered cars in 2009, and funding for fuel-cell research was cut in favor of plug-in electric vehicles, as Obama set a goal of having 1 million electric vehicles on the road by 2015 [Angela Greiling Keane and Alan Ohnsman, 2012].

Nonetheless, fuel cells are now starting to enjoy good moments, and given their number of already mentioned advantages over other technologies this will increasingly be the case. However, considering some skepticism that surround them, mainly due to delay in their commercialization, their profitability in this early market may play a crucial role to their success in the years to come.

The cost of automotive fuel cell systems has been drastically reduced from the values of 2002 of about \$275/kW to \$49/kW in 2011, assuming a high volume pro-

duction of 500 000 units per year [U.S. Department of Energy, 2012]. This needs to further be reduced in order for fuel cells to commercially compete with the current technology of Internal Combustion Engines (ICEs), which costs as low as $25 - $35/kW. The cost target of $30/kW was initially set for 2015 by DOE, but then has been postponed to 2017 in their latest technical-plan report. The target includes also the achievement of a durability target of 5000 hours for their commercialization, which is the equivalent of the average durability of ICE.

Consequently, many of the major auto-makers along with DOE continue to project initial commercial production in 2015, with Hyundai and Toyota planning to sell at $50 000, and other big players in the industry, GM, Honda, Daimler and Mercedes among others committed to similar goals [U.S. Department of Energy, DOE, 2011]. Therefore, one could argue that the long anticipated promises are recently starting to be met, considering also the number of fuel cell buses and fleets of Fuel Cell Electric Vehicles (FCEVs) that are already being tested in different regions of the world.

1.4.2 Stationary Application

Table 1.2: Commercially available large stationary fuel cells in 2011. Source: Breakthrough Technologies Institute Inc. [2012]

Table 8: Commercially Available Stationary Fuel Cells 2011			
Prime Power and mCHP			
Manufacturer	**Product Name**	**Type**	**Output**
Ballard	FCgen-1300	PEM	2 – 11 kW
	CLEARgen	PEM	Multiples of 500 kW
Bloom Energy	ES-5400	SOFC	100 kW
	ES-5700	SOFC	200 kW
Ceramic Fuel Cells	BlueGen	SOFC	2 kW
	Gennex	SOFC	1 kW
ClearEdge Power	ClearEdge 5	PEM	5 kW
	ClearEdge Plus	PEM	5 – 25 kW
ENEOS CellTech	ENE-FARM	PEM	250 – 700 W
FuelCell Energy	DFC 300	MCFC	300 kW
	DFC 1500	MCFC	1,400 kW
	DFC 3000	MCFC	2,800 kW
Heliocentris Fuel Cells AG	Nexa 1200	PEM	1.2 kW
Horizon	GreenHub Powerbox	PEM	500 W – 2 kW
Hydrogenics	HyPM Rack	PEM	Multiples of 10, 20, and 30 kW
	FCXR System	PEM	150 kW
Panasonic	ENE-FARM	PEM	250 – 700 W
Toshiba	ENE-FARM	PEM	250 – 700 W
UTC Power	PureCell Model 400	PAFC	400 kW

Continuing in the wide spectrum of fuel cell applications, the stationary sec-

tor is one that is growing very rapidly and has already its early success stories. Stationary applications can be *small* as in the case of Uninterrupted Power Supply (UPS), backup powers and remote powers or *large*, as prime power plants for data centers and μ-CHP for residential households and commercial buildings. Low and high temperature Proton Exchange Memebrane (PEM) fuel cells can supply both small and large stationary applications, while MCFCs, Solid Oxide Fuel Cells (SOFCs) and Phosphoric Acid Fuel Cells (PAFCs) are mainly used for large stationary applications.

Table 1.3: Commercially available small stationary fuel cells in 2011. Source: Breakthrough Technologies Institute Inc. [2012]

Manufacturer	Product Name	Type	Output
Altergy Systems	Freedom Power System	PEM	5 – 30 kW
Ballard	FCgen 1020A CS	PEM	1.5 – 3.6 kW
ClearEdge Power	ClearEdge CP	PEM	10 kW
Dantherm Power	DBX 2000	PEM	1.7 kW
	DBX 5000	PEM	5 kW
Horizon	H-100	PEM	100 W
	H-1000	PEM	1 kW
	H-3000	PEM	3 kW
	H-5000	PEM	5 kW
	MiniPak	PEM	100 W
Hydrogenics	HyPM XR Power Modules	PEM	4, 8, and 12 kW
IdaTech	ElectraGen H2-I	PEM	2.5 - 5 kW
	ElectraGen ME	PEM	2.5 - 5 kW
Microcell	MGEN 1000	PEM	1 kW
	MGEN 3000	PEM	3 kW
	MGEN 5000	PEM	5 kW
ReliOn	E-200	PEM	175 W
	E-1100/E-1100v	PEM	1.1 kW
	E-2500	PEM	2.5 kW
	T-1000	PEM	600 W – 1.2 kW
	T-2000	PEM	600 W – 2 kW
SFC Energy	EFOY Pro Series 600, 1600, 2200	DMFC	25, 65, and 90 W

There are a number of commercially available stationary fuel cells, and many companies are selling their fuel cell systems. Some of these are given in Tab. 1.2 and Tab. 1.3. The Japan's Ene-farm scheme is one of the most successful fuel cell programs to date, which was planned since the 1990's and was launched in 2005. It is a fuel cell residential μ-CHP program mainly dominated by PEMFCs, with recent introduction to the program of SOFCs. Since the start of commercialization in 2009, 20 000 units were sold until 2011 and the sales of the same number of units are expected in 2012 alone [Carter, 2012].

Recently, there is a tendency by renowned internet companies to replace part of the power supply for their data centers with fuel cell installations. Google was

the first to deploy Bloom Energy fuel cells in 2008 with 400kW installation at their Mountain View, California headquarters. Then, eBay started in 2009 with 500kW installation and have recently announced their plan for 6MW installation for their data center in Salt Lake City, Utah to be operational by mid 2013 [Bloom Energy, 2012]. Apple is also planning to deploy 5MW installation in Maiden, North Carolina, where the iCloud data centers are located [Apple Inc., 2012]. This tendency that more and more internet companies and services rely on fuel cells for powering their data centers is a sign that among their other advantages fuel cells are proving to be reliable power sources.

1.4.3 Portable Application

Portable application of fuel cells include, Auxiliary Power Units (APUs), methanol fuelled battery chargers, toys, etc. Direct Methanol Fuel Cells (DMFCs) are the main candidates for this application, even though miniaturization of PEMFCs is also making them increasingly interesting for portable applications. However, miniaturization is still a challenge, reason for which development of fuel cells for such applications as mobile phones and laptop computers is still slow compared to the other applications mentioned above. Many fuel cell patents have been filed by Samsung and Apple recently [Lohr, 2012; Spare; Bradley L. ; et al., 2010], which may be an indication that the days when we will be able to use consumer electronics powered by fuel cells are drawing ever closer.

Summary

This chapter has introduced the concept and working principles of fuel cells and the role they can play in the future of energy systems. Given the number of advantages over other energy sources that include versatility and fuel flexibility, and considering also the urgency for shift in trend towards greener sources of energy, the role of fuel cells is crucial for a global energy system that considers the environmental and socio-economic advantages to our societies.

The work that is being done in the field in many parts of the globe, summarized in this chapter, is a glimpse of a greener future. The gap between now and this future is the main drive of the current research work, where a better fundamental understanding of the degradation mechanisms in a fuel cell is the first and necessary step for making them more durable and reliable.

2 High Temperature PEM fuel cells

This section gives the motivation for the current work and states the main objectives. After introducing the fuel cell type under investigation, a high temperature PEM fuel cell, and describing the working principles, it presents its different components. Knowing these components and how they are assembled to work together is crucial for understanding their degradation modes, which are also provided together with possible characterization methods as part of the literature review for this research project.

2.1 Background

2.1.1 Motivation for the Current Research Project

A proton exchange membrane or polymer electrolyte membrane fuel cell (PEMFC) is a type of fuel that is normally classified as low-temperature fuel cell and employs a solid polymer as an electrolyte as the name suggests. Since its invention in the early '60s a number of PEM based variants of fuel cells have been introduced. Among them are PEM–based direct alcohol fuel cells, such as DMFC and Direct Ethanol Fuel Cell (DEFC). To date, PEMFCs top many lists in the fuel cell arena, from the most sold in this early market stage to the most researched fuel cells, and consequently, they enjoy the most investment shares compared to other types of fuel cells [Fuel Cell Today, 2011].

The fuel cells under investigation in this research project can be considered as the technological off springs of PEMFCs, whose only difference consists on the type of polymer electrolyte they employ. They make use of acid-based polymer instead of a water-based one to operate at temperatures above $100\,^{\circ}\mathrm{C}$, hence, known

as High Temperature Proton Exchange Membrane Fuel Cells (HT-PEMFCs). Since their invention in 1995 by Wang et al. [1996], they have drawn much attention as they resolve some of the issues related to their low temperature counter parts. They bring about cost reduction and reliability in terms of improved reaction kinetics, catalyst tolerance to impurities such as CO, heat rejection, and water management with respect to PEMFC, which operates at temperatures lower than 100 °C.

HT-PEMFCs not only resolve some of the problems associated with low temperature PEM fuel cells, but also open new opportunities to the technology development in the field. Easier or no water management and easier heat rejection means simpler design, and tolerance to CO combined with useful excess heat gives opportunities for using reformer systems, internal or external, to feed the fuel cell with hydrogen from the reforming of hydrocarbon, such as natural gas, gasoline, methanol or ethanol. This is convenient as it eliminates the hydrogen storage problems and the need for a new infrastructure for the distribution and supply of hydrogen. All these advantages from simpler design to integration with reformers could translate into cost reduction, making HT-PEMFCs increasingly attractive for use both in transportation application [Martin and Wörner, 2011; McConnell, 2009] and stationary applications, like micro–Combined Heat and Power (μ–CHP) co-generation applications [Andreasen et al., 2011; Arsalis et al., 2013; Li et al., 2009]. They are also suitably used for mobile and semi-stationary power supplies, and for reliable stationary or portable backup power for a variety of applications; such as servers, hospitals, and telecommunication.

Despite their numerous advantages, wide commercialization of HT-PEMFCs still face hindrance due to durability and degradation issues that are not yet well described. Cost is another challenge that is being addressed in many ways, especially by decreasing the Pt catalyst loading and looking into non-noble metals as catalyst materials to replace Pt. Therefore, the challenges surrounding real life operation, such as durability and cost viability issues, are some of the last obstacles to their full commercialization.

Denmark is continuously and extensively investing in fuel cell research to resolve these challenges, as part of its plan for 100% fossil independence by the year 2050 [Danish Partnership for Hydrogen and Fuel Cell, 2012; Hydrogen Link Denmark Association, 2012]. This is based on a strong partnership and cooperation among companies and research institutions. Research and development in HT-PEMFCs is done in companies such as Serenrgy A/S, Danish Power Systems; and the country's major research institutions, like the Technical University of Copenhagen (DTU) and Aalborg University (AAU).

This project thoroughly investigates the degradation and durability issues in such fuel cells, especially in the presence of methanol reformate impurities. Therefore, the motivation for the current work can be summed up as the pursuit of a clean energy future and bet on the potential that fuel cells have to help meet such ambition.

2.1.2 Definition of Research Objectives

The objective of this dissertation is to characterize the main mechanisms that control the performance and degradation issues in HT-PEMFCs. It addresses their response to non-optimal operating conditions that are expected during real life operation of the cell, such as the presence of impurities of various types in the anode feed. It investigates these issues, both from literature assessments and from experimental tests by means of Electrochemical Impedance Spectroscopy (EIS), which is described in section 2.4. The project aims at understanding the fundamentals of the degradation modes by also relating the degrading factors to each other.

In light of the motivation for the current research project, the objective is to contribute in making durable and cost effective HT-PEMFCs. Understanding the underlying mechanisms of degradation is key to achieving these goals, and therefore, fundamental experimental characterization has been done in this work.

2.2 Fundamentals of HT-PEMFC

Except for the elevated temperature, typically between 160–180 °C, an HT-PEMFC operates similarly as a PEMFC and the same half-cell reactions govern the working principle. This principle is illustrated in Fig. 1.2. Hydrogen is fed on the anode side and oxygen or air on the cathode side, where hydrogen oxidation and oxygen reduction reactions then take place in the respective electrodes to produce electricity, heat and water vapor. Due to the elevated operating temperature involved water is no more a suitable proton conduction media as it is not present in liquid form at the favorable atmospheric pressure operation. This leads to the substitution of the usual PEMFC membrane, Nafion®, whose proton conductivity highly depends on the presence of liquid water, with another membrane based on PBI. PBI, if doped in Phosphoric acid, which is proton conductive in the absence of water, can conduct protons and ensure high efficiency at high temperatures and therefore be suitably used in an HT-PEMFC.

The degradation of fuel cell performance or its failure is normally caused by the degradation of its components. Therefore, understanding the parts of a fuel cell and how they function together is crucial for characterizing the degrading mechanisms in a fuel cell. For this, the main parts of an HT-PEMFC are briefly described below. Further down, their degradation modes and possible characterization tools are given.

2.2.1 The Making of a Single HT-PEMFC

A single HT-PEMFC assembly is an onion layering of repeating units on both sides of the electrolyte membrane, which is the central part. The heart of a fuel cell, crucial for all the electrochemical processes within the cell is a thin layer called Membrane Electrode Assembly (MEA). It is sandwiched between two flow plates that allow the flow of reactant gases, both to the anode and the cathode sides of the

MEA. The flow plates are then sandwiched between a pair of current collectors that are connected to an external load or a device for harnessing the electricity produced by the chemical reactions within the fuel cell. An exploded view of the central part of an HT-PEMFC single cell assembly is shown in Fig. 2.1.

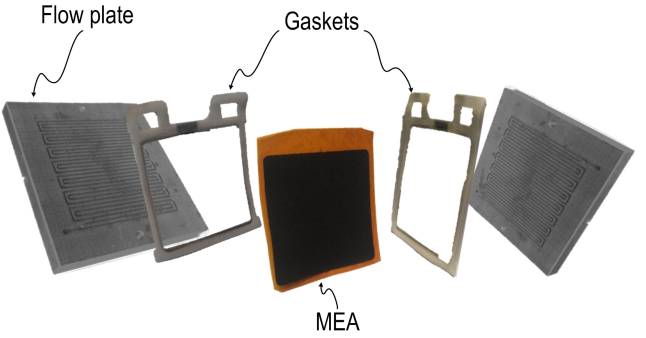

Figure 2.1: The central part of an HT-PEMFC single cell assembly where flow of gases and chemical reactions take place.

Membrane Electrode Assembly (MEA)

From an electrochemical point of view the MEA is the core of the fuel cell, since here is where all the relevant reactions take place. It is composed of the polymer electrolyte membrane, PEM, sandwiched between the two electrodes. The electrolyte membrane has to efficiently conduct protons as exclusively as possible. Other functions of the membrane include blocking the gaseous reactant from migrating from one electrode to the other while acting as an interface for the respective half-cell reactions of the reactant gases. Moreover, it serves as a support for the catalyst and electrically isolates the two electrodes.

Li et al. [2009] identify four groups of membranes for HT-PEMFCs, namely: (1) modified Perfluorosulphonic Acid (PFSA) membranes; (2) alternative membranes based on partially fluorinated and aromatic hydrocarbon polymers; (3) inorganic–organic composites; (4) acid–base polymer membranes. H_3PO_4-doped PBI, an acid–base polymer membrane is the most commonly used in HT-PEMFCs, and is increasingly dominant due to its specific properties for operation at temperatures up to 200 °C. These properties as listed by Savinell's group, the ones that hold the first patent [Savinell and Litt, 1998] on the casting of H_3PO_4–doped PBI membrane, include; good protonic conductivity at elevated temperature, near zero electro-osmotic drag, which means that the proton conduction through these membranes do not involve water transport, low gas permeability, and low methanol crossover [Wainright et al., 1995]. To these other advantages can be added, such as good thermal stability with a gas transition temperature (T_g) of around 425 °C– 436 °C [Li et al., 2004], mechanical and chemical stability and low cost. The basic chemical structure of a PBI repeat unit is shown in Fig. 2.2.

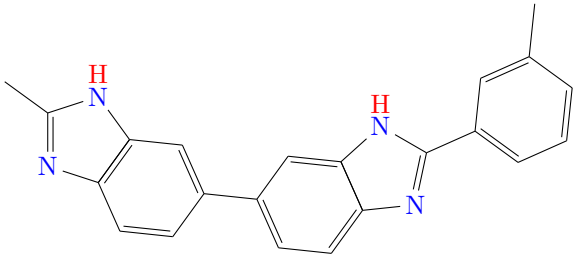

Figure 2.2: Chemical structure of a PBI repeat unit.

In addition, the MEA consists of the electrodes, which are found on both sides of the polymer membrane, anode on one side and cathode on the other. The electrodes are composed Gas Diffusion Layer (GDL) and the Catalyst Layer (CL). The GDL is made of an outer macro-porous carbon fiber layer and an inner carbon-based Mirco-Porous Layer (MPL) for the flow of the gaseous reactants. The GDL serves also for electric contact with the flow plates. The CL is the reaction site, in which Pt nano–particles are dispersed on a carbon support, or coated/sprayed on the MPL itself. The Pt particles are usually mixed with ionomers that serve as binders in the electrodes, and for proton conduction to the membrane.

The MEAs that are used in this research project are Celtec®–P MEAs from BASF. They are produced by direct casting from poly-phosphoric acid solution followed by hydrolysis in water and then by a sol-gel transition to form PBI membranes with high acid content [Calundann, 2006].

Flow Plates

The Flow plates are the flow patterns through which reactant gases flow towards MEA. They are multifunctional and therefore, they have to fulfil high electrical conductivity, low gas permeability, high corrosion resistance, sufficient strength, low thermal resistance, and low cost, etc.The most common materials used for flow plates are carbon graphite or graphite polymer, and even metals such as Al, Ti, and Ni [Wu et al., 2008]. They are present on both sides of the MEA to allow the flow of reactant gases to the GDL from their respective inlets. In a fuel cell stack assembly the plates separate two adjacent cells and block the flow of gases while conducting the electric current between them.

Gaskets and Other Seals

The gaskets and other seals are used to prevent the leaking of reactant gases and coolants. Even though they do not constitute a major concern from a degradation point of view their correct sizing is crucial for optimal sealing. They are usually made of silicon rubber, and in addition to sealing they also serve as electrical insulators between the parts they separate.

2.3 Degradation Of HT-PEMFC

2.3.1 Energy Carriers & Degradation

Fuel flexibility is one of the major advantages of fuel cell technology compared to other technologies. However, the durability of an HT-PEMFC depends on the energy carrier used as a source of hydrogen and the method used for obtaining it. Hydrogen, even though not readily available on the earth's atmosphere in its molecular state, it is found in a variety of forms as a constituent of many molecules; hydrocarbons, alcohols, and water. All these represent primary fuel sources for the so called '*hydrogen economy*' [W. Crabtree et al., 2004].

The process of hydrogen production depends on the type of the primary source used, which consequently determines the quality grade of the H_2 gas obtained. Current options include the reforming of hydrocarbons and alcohols; gasification of coal and biomass; and the splitting of water by water-electrolysis, photo-electrolysis, photo-biological production and high temperature decomposition [IEA, 2007]. Presently, most of the hydrogen for industrial purposes is produced by steam reforming of natural gas or methane [marketsandmarkets.com, 2011].

The electrolysis of water is a simple process in which electricity is used to split water into its constituents, H_2 and O_2. The process gives pure H_2, which is highly desired for use in PEM and HT-PEM fuel cells since they involve Pt electrocatalyst, sensitive even to trace impurities [Du et al., 2009; Li et al., 2003, 2009]. The issue with using electricity to produce H_2 gas at the moment is the dominance of non-renewable sources for its production. However, if excess electricity from PV, wind energy or even hydroelectric energy is available, the process can be a viable source of pure and environmentally friendly H_2 gas for fuel cells [Honnery and Moriarty, 2009; Silva et al., 2005].

The steam reforming of hydrocarbons and alcohols on the other hand requires steam and heat and provides a hydrogen rich mixture of gases called *reformate*, which contains traces of impurities. While this has the advantage of on site hydrogen production and that liquid alcohols can use existing distribution infrastructures, as already mentioned, the trace impurities have degrading effects on an HT-PEMFC.

Even in the case of steam reforming, for the process to be CO_2 neutral, the fuel and the heat should be provided by renewable means. Methanol, with lower reforming temperature has the possibility of being CO_2 neutral if produced from renewable sources such as wood, forest waste, peat, municipal solid wastes, sewage and even chemical recycling of CO_2 in the atmosphere [Bromberg and Cheng, 2010; Olah et al., 2009]. This however, does not eliminate the degradation issues associated with the reformate impurities.

2.3.2 Durability

Durability and lifetime tests are the main ways of validating a technology, and consequently vital for the development of new devices, such as fuel cells that are

supposed to replace existing ones. Fuel cells are candidates to replace combustion engines for cleaner energy generation and to replace or work in complementarity with batteries for faster refueling, higher energy density and longer operation time. Therefore, reliability, durability and stability are necessary conditions for their full deployment. Reliability is defined as the ability of a fuel cell or stack to perform the required function under stated conditions for a period of time; durability is the ability of a fuel cell or stack to resist permanent change in performance over time; and stability is the ability to recover power lost during continuous operation [Wu et al., 2008].

Correspondingly, the minimum requirement the DOE has set for the commercialization of FCEVs is that the fuel cells that power them should be as durable and reliable as today's ICEs, which can last for as long as 5000 hours operating lifetime. More precisely they must be able to perform over the full range of operating temperatures ($-40\,^{\circ}$C to $40\,^{\circ}$C) with less than 10% loss of performance at the end of life. So far, DOE has reported durability of around 2500 hours with cycling for net 80kWe integrated transportation fuel cell power systems operating on direct hydrogen. Fuel cell buses however, have achieved more than 10 000 operating hours in real-world-service with the original cell stacks and no cell replacement [U.S. Department of Energy, DOE, 2011].

For stationary applications operating lifetimes of more than 80 000 hours are required. Similarly to automotive applications the end of life is designated when 10% loss of performance is reached. Even in this case the fuel cell must be able to perform over the full range of external environmental conditions ($-40\,^{\circ}$C to $40\,^{\circ}$C), a target that has already been achieved by PAFC installations [U.S. Department of Energy, DOE, 2011]. HT-PEMFCs being suitable both for automotive and stationary applications have to meet both durability targets under the specified respective stress conditions.

2.3.3 Degradation Modes

The degradation modes in an HT-PEMFC can be thermal, chemical and/or mechanical. These mechanisms are related to each other and entangled in their causes and effects, which sometimes makes it difficult to distinguish between them. For-example, higher operating temperatures usually enhance the rates of chemical reactions and therefore that of the chemical attacks, which in turn can cause weakening of the parts and make the fuel cell more vulnerable to mechanical and thermal stresses.

The flowchart in Fig. 2.3 summarizes the different stress factors that lead to different degradation mechanisms, and the different parts of an HT-PEMFC that are attacked. Wherever possible, the techniques to measure the effects are given in brackets. It can be noticed that higher operating temperature is involved in most of the degradation mechanisms, and that most of the mechanisms lead to loss of Electrochemical Surface Area (ECSA). The figure also gives an idea of the complexity from a characterization point of view of the degrading mechanisms and their causes and effects.

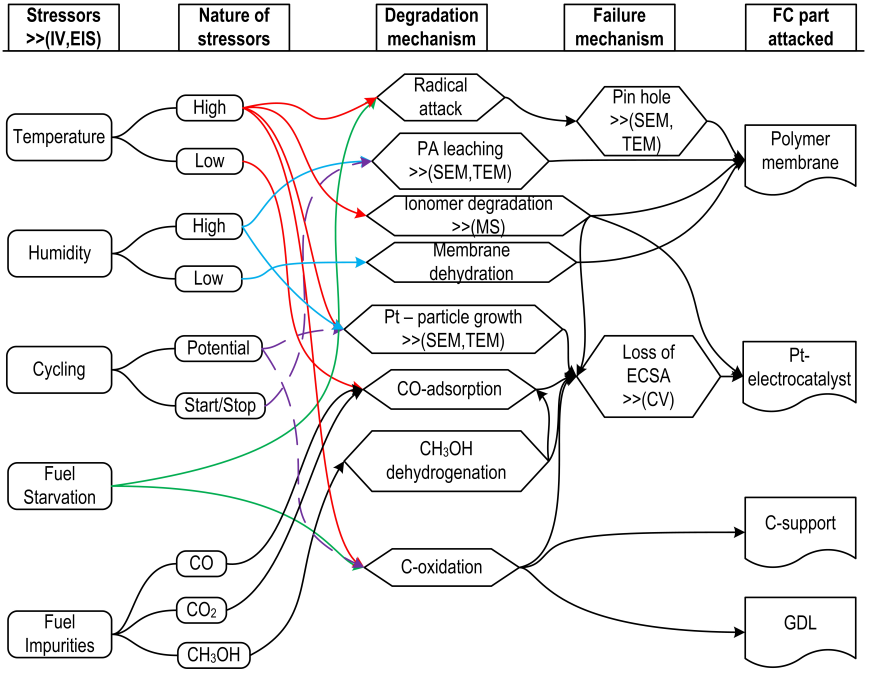

Figure 2.3: HT-PEMFC Degradation flowchart

Therefore, it is more suitable to classify degradation mechanisms based on the parts of the fuel cell they occur in, since they differ from one part to the other due to the different nature of the materials used. The main parts that cause performance degradation or even fuel cell failure if degraded are the polymer electrolyte membrane, the Pt catalyst and the carbon support of the Pt catalyst. The GDL also has a significant impact on the fuel cell performance if degraded, however, being made of carbon its degradation mechanisms are similar to that of the carbon support. The possible degradation mechanisms for each of these components are given below.

Membrane Degradation

As already introduced, HT-PEMFCs mainly employ H_3PO_4/PBI–based membrane. Membrane degradation mechanisms at HT-PEMFC operating conditions are not yet well described, but similar mechanisms at a faster rate with respect to those seen in Low Temperature Proton Exchange Memebrane Fuel Cells (LT-PEMFCs) are expected, due to the increased operating temperature. For-example, crossover may cause H_2 and O_2 to react on the membrane surface generating hotspots, which may lead to pinhole formation. Membrane thinning can also increase the chances for pinhole formation, which in turn causes increased fuel crossover [Schmidt,

2006]. Membrane thinning can be accelerated by high temperature, ionomer loss, Open Circuit Voltage (OCV) operations and carbon corrosion [Schmidt and Baurmeister, 2008; Zhang et al., 2009].

Chemical instability due to peroxide (H_2O_2) and radical ($^{\bullet}OH$ or $^{\bullet}OOH$) attack is a common concern to the life time of PEMFC, with potentially more aggressive effects at higher operating temperatures [Li et al., 2009]. These peroxy radicals are formed inside the fuel cell due to the reactants crossover and consequent reactions on the Pt surface [Borup et al., 2007].

All the above mentioned mechanisms lead to loss in mechanical stability, due to membrane thinning or pinhole formation that can lead to the formation of cracks and fractures. This concerns are even more at higher operating temperatures, which makes them real challenges in the case if an HT-PEMFC [Zhang et al., 2006]. They are challenges also because the requirements for mechanical stability are usually opposite to those for an effective proton conductivity. For-example, thicker membrane is more robust mechanically, but the proton conduction capabilities decrease with increase in membrane thickness. Acid-doping level also affects conductivity and mechanical strength oppositely [Li et al., 2009].

If phosphoric acid, which is the proton conduction media in PBI–based MEAs is removed, the proton conductivity of the membrane obviously decreases. This removal is observed from the cathode side at higher operating temperatures (180 °C–190 °C) [Yu et al., 2008]. The same study also showed that PA leaching is not a major factor in reducing the MEA's lifetime by showing that only small percentage of H_3PO_4 was lost after more than 10 000 hours of operation. The flow plates can also squeeze out the acid and absorb some of it from the MEA. However, acid loss mechanisms and PA mobility inside a PBI–based MEA and the effects, especially under reformate operation, are not yet fully understood.

Catalytic Degradation

Most commonly used catalyst in HT-PEMFCs is carbon supported Pt, and its degradation is the most important degradation in HT-PEMFCs. It is manifested by Pt particle agglomeration according to Ostwald ripening process, where the growth of particle size is caused by the Pt dissolution and re-deposition [Song et al., 2008]. This growth in particle size reduces the ECSA of the catalyst, thereby causing the performance degradation of the fuel cell. The kinetics of this process increases with the increase in temperature causing it to be more severe in HT-PEMFCs than in LT-PEMFCs. Liu et al. [2006] reported that rapid growth of the Pt particles occurred in the presence of H_3PO_4 and high temperature environment implying that such an environment speeds up the process of Pt dissolution and re-deposition.

Surface coverage by adsorbed impurities is another mechanism that causes loss in the performance of Pt electro-catalyst-based fuel cells. However, this is a degradation mechanism whose negative effects decrease with increase in temperature. Among other impurities the preferential adsorption of CO on Pt surface is of major concern [Du et al., 2009; Li et al., 2003].

In the case of methanol-based reformate, methanol electrooxidation on Pt surface can cause performance loss and lifetime issues. It oxidises both via direct and indirect routes, that involve the formation of CO_{ads}, and other intermediates such as formaldehyde and formic acid [Cao et al., 2005; Iwasita, 2002]. The intermediate formations could act as catalyst poisons. Moreover, the rate of this oxidation is reported to increase with increase in temperature [Modestov et al., 2012], making HT-PEMFCs more susceptible to such degradation mode.

Carbon Support Degradation

Carbon corrosion is a slow reaction at low temperature, making carbon a suitable catalyst support for LT-PEMFCs. However, carbon corrosion is a function of temperature among other factors, and it has been shown that it accelerates at higher temperature operations ($\sim$200 °C) [Schmidt, 2006; Song et al., 2008].

Schmidt and Baurmeister [2008] observed that the main effect from carbon corrosion is an increase in the hydophilicity of the cathodic catalyst layer concomitant with electrolyte flooding which, in turn, leads to increase of the cathode mass transport overpotentials.

Carbon corrosion weakens also other parts than the carbon support itself. It weakens the Pt catalyst it is supposed to support and causes loss of ECSA that translates in performance loss. It also weakens the membrane by causing its thinning, which can lead to increased fuel crossover and pinhole formation [Schmidt, 2006].

Material degradation therefore, remains one of the main issues in HT-PEMFCs, especially due to the challenge of increased operating temperatures. Since understanding the modes of degradation is the first step to mitigating them, characterization tests are necessary for the development and deployment of HT-PEMFC fuel cells. In the following section some characterization techniques relevant to the study of HT-PEMFCs are discussed.

2.4 HT-PEMFC Characterization Techniques

Although, the development of computational models and simulations that can give a detailed characterization at unit cell and stack levels are crucial, they need to be verified and validated through experimental results. Therefore, detailed and at the same time non-intrusive characterization methods are needed for testing real life operating conditions.

A number of characterization methods are used in fuel cell research. They can be *in-situ*, where tests are performed on a running fuel cell, or *ex-situ*, in which only parts of a fuel cell are tested separately. Common in-situ characterization techniques include [Ryan O'Hayre, 2004]; Current–Voltage measurement (Polarization curve), EIS, Cyclic Voltametry (CV), analysis of effluents, etc. Among

the ex-situ techniques Microstructural characterization via microscopy, Nuclear Magnetic Resonance (NMR), Energy-Dispersive X-ray Spectroscopy (EDS) and Porosimetry can be mentioned [de Bruijn et al., 2008; Guilminot et al., 2007; Iojoiu et al., 2007; Jian et al., 2002].

The different methods are usually used to characterize different parts or phenomena in the fuel cell and are usually complementary with each other. Therefore, if used in conjunction to each other, they can help to identify the different processes and mechanisms that lead to the fuel cell's degradation. Some of the methods that are relevant for the characterization of HT-PEMFCs are described below.

2.4.1 Electrochemical Impedance Spectroscopy (EIS)

Impedance spectroscopy, also known as Electrochemical Impedance Spectroscopy (EIS) or AC impedance, is a technique of characterization of electrochemical devices. It is done by measuring the electrical response of a material to small induced signal perturbances. These are then analyzed to obtain useful information about the behavior of the device under various conditions.

Impedance, like resistance, is a ratio of voltage and current, quantifying the ability of a substance to block the flow of current through it, with the only difference being that the voltage and current are time dependent in the case of impedance. This makes impedance a complex function that can be calculated by Eqn. (2.1), using the amplitudes of the current, the voltage and the phase shift;

$$Z = \frac{V_0\, e^{j(\omega t - \phi)}}{I_0\, e^{j\omega t}} = \frac{V_0}{I_0}\, e^{-j\phi} = Z_0\left(\cos\phi - j\sin\phi\right). \tag{2.1}$$

In Eqn. (2.1), Z [Ω] is the complex impedance response of the system, V_0 [V] and I_0 [A] are the voltage and current signal amplitudes respectively, ω [rad/s] is the signal frequency and ϕ [rad] is the voltage phase shift. It has a real part ($Z_0 \cos\phi$) and imaginary part ($Z_0 j \sin\phi$), and is normally represented on a Nyquist curve with real part on the horizontal axis and the imaginary on the vertical axis. Typically in a Nyquist plot the imaginary axis is inverted for a more familiar 4^{th} quadrant representation, and higher frequency measurements are found closest to the origin, decreasing from left to right on the quadrant. A typical idealized Nyquist plot of an HT-PEMFC is shown in Fig. 2.4.

In fuel cells, EIS was recently used extensively for optimization, characterization and diagnostics [Andreasen et al., 2011; Asghari et al., 2010; Fouquet et al., 2006; Mamlouk and Scott, 2011; Pattamarat and Hunsom, 2008; Yuan et al., 2010; Zhang et al., 2009]. The different processes that occur in a cell respond differently to perturbances at different frequencies. If a fuel cell is perturbed on a broad range of frequencies, at low frequency the effects on slower processes with longer time constant like diffusion will be registered, and at higher frequency effects of faster processes such as charge transfer would be sensed. The technique is described in detail in [Barsoukov and Macdonald, 2005; Orazem and Tribollet, 2008] for general application and in [Yuan et al., 2010] for PEM fuel cells in particular.

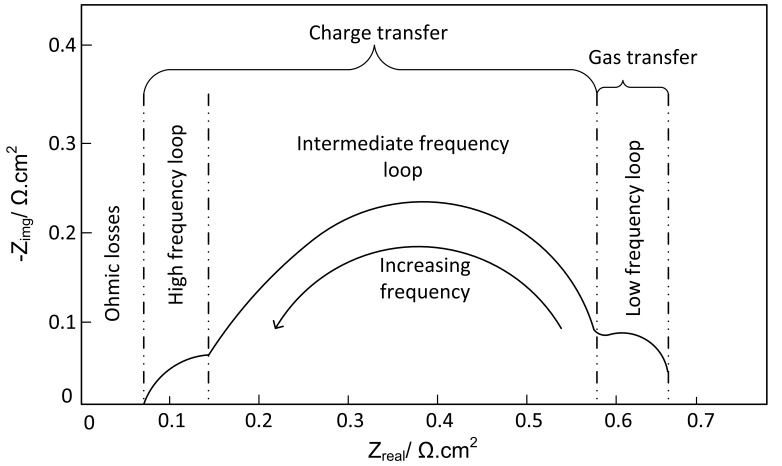

Figure 2.4: A typical idealized Nyquist plot of HT-PEMFC.

One of the main advantages of EIS is that it is not intrusive and can be performed *in-situ*. It is a detailed technique with which information about different processes in the electrochemical device can be obtained with only little perturbation. Since the perturbances are very small compared to the measured DC voltage or current, changes within the cell are minimal [Monk, 2007]. In a PEM fuel cell an AC perturbance of $\sim 5\%$ of the measured DC value can be suitably used [Yuan et al., 2007].

In order to translate impedance measurement in to more comprehensible figures and extract meaningful information, the analysis of data is typically done by fitting the measured data to an Equivalent Circuit (EC) or a model based on physical properties that can reasonably represent the fuel cell under investigation. An EC model is a network of ideal circuit elements, such as resistances, capacitances and sometimes also inductances that are arranged in a way that they can reproduce the impedance of the electrochemical device. A typical EC model for an HT-PEMFC is given in Fig. 2.5. Even though, the correspondence between the different circuit elements and loops in an EC model and the fuel cell parts are still controversial, it is useful to see this representation of what part of the fuel cell contributes the most to what part of the EC model.

2.4.2 Potential Sweep Methods

Polarization curve, also known as *I-V* curve, is the most common way of representing the performance of a fuel cell quantitatively. The term polarization implies loss, voltage drop in this case, and therefore a polarization curve shows the losses of a fuel cell with the increase in current density. The different losses that can be identified in an *I-V* curve are, activation losses, ohmic losses and mass transport losses (also known as concentration losses). They are presented in an *I-V* curve

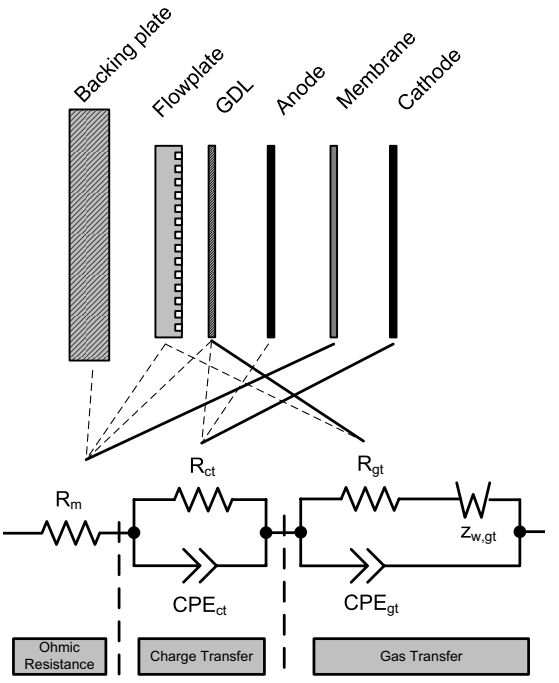

Figure 2.5: Equivalent circuit model for HT-PEMFC: *Reproduced from Jesper Lebæk [2010]*.

in that same order as they happen with increasing current density. Though not as sophisticated and detailed as EIS, *I-V* curve can give a general idea of performance profile of a fuel cell and is easier to perform and analyze. For this it is widely used in fuel cell research to investigate the response of a fuel cell to change in operating condition, such temperature, pressure, Pt-loading, presence of contaminants, or merely the effects of time [Li et al., 2003; Liu et al., 2006; Schmidt, 2006].

Another commonly used potential sweep method is Cyclic Voltammetry (CV) [Higier and Liu, 2012; Wu et al., 2008]. It is done by ramping the potential of a fuel cell to a certain value and back to the starting point. The corresponding current is then recorded and two peaks are registered, a positive current peak for the anodic oxidation and a negative one for the cathodic reduction. The information that can be obtained from such method is usually the surface coverage by absorption of the electro-active catalyst area (loss of ECSA). Measurements are taken at different instances, before and after operation in the presence of contaminants, and the active surface areas at those instances are compared.

CV was shown to be useful in CO adsorption/oxidation tests [Cheng et al., 2007; Sethuraman et al., 2009]. In PBI–based fuel cells, it has been used to investigate the effects of temperature and OCV on the performance and degradation and

in continuous aging tests [Hu et al., 2006; Lobato et al., 2007; Qi and Buelte, 2006; Zhang et al., 2007].

2.4.3 Analysis of Effluents

The composition of the anode and cathode effluents can give information regarding the possible electrochemical processes in a fuel cell. Evolution of some gases, such as CO, CO_2, and O_2 can be detected and be used to characterize degradation mechanisms. Moreover, ionomer degradation species can be detected by analyzing the cathode and anode effluents [de Bruijn et al., 2008].

Acid loss is an important aspect of HT-PEMFC degradation that can be analyzed by this method. Another application could also be to determine the permeability to some impurities of the polymer membrane. Effluents can be analyzed by different methods of gas analysis, such as Mass Spectroscopy (MS), Fourier Transform InfraRed (FTIR), Gas Chromatography (GC), etc.

2.4.4 Microstructural Characterization

Another technique that is usually used as a post-mortem analysis in durability tests is the microstructual analysis of the MEA. This can reveal the structural changes in the Pt catalyst, i.e., Pt particle dissolution and redeposition. Mechanical degradations, such as creeps and microfractures in the membrane and other parts of the MEA can also be revealed by this kind of characterization.

These are usually *ex-situ* characterization techniques done to compare the state of the MEA before and after degradation or durability tests. Sophisticated techniques of microscopy, like SEM and Transmission Electron Microscopy (TEM) are used for these purposes. PBI membrane and the MEA structure were analyzed by TEM and SEM in HT-PEMFCs [Hu et al., 2006; Kongstein et al., 2007; Liu et al., 2006; Seland et al., 2006]. Furthermore, NMR can be used to analyse the chemical composition of the ionomer in anode and cathode after operation and EDS can be used to study morphological changes that occur during aging [de Bruijn et al., 2008; Guilminot et al., 2007; Iojoiu et al., 2007].

Summary

In summary, there are clear advantages in operating a PEMFC at temperatures of above 100 °C, including improved kinetics and improved tolerance to impurities, like CO. However, there also challenges related to high temperature operation, mainly accelerated kinetics of some chemical, thermal and consequently mechanical degradation modes. The objective of this work is to understand the underlying mechanisms of the various degradation modes in an HT-PEMFC, which is a crucial path to their mitigation and the design and development of more durable fuel cells.

From what is presented in this chapter it can be said that, the different stress factors affect different parts of the fuel cell in different modes. The level of stress due to impurities depends on the quality grade of the hydrogen gas used, which in turn depends on the source and the means of hydrogen production. Moreover, the different degradation mechanisms are related to each other in complex ways, making it difficult to distinguish among the various causes and effects. In the following chapters, the methodology used in the current work followed by the results obtained and their analysis and interpretations, are presented.

3 Methodology

This section describes the fuel cell test station that is used in the current work. Since vapor impurities of reformate gas are also the object of the current work, a dedicated vapor delivery system that is employed in the experimental setup and the steps of its preparation are described in this section.

3.1 Introduction

Generally speaking, research in fuel cells lacks of standardized test protocols that can be found for almost all other established technologies. Part of the reason for this difficulty of standardizing test protocols, which if done properly would lead to the uniformity and comparability of different tests, could be attributed to the fact that fuel cells are operated in a wide range of conditions and for a variety of application, like no other technology before. Another reason is attributable to the fact that the effects of some conditions are not yet thoroughly investigated and hence not well described to have a standardized test protocol.

Nevertheless, even though not standardized, there are a number of test protocols, issued by various organizations, mainly the EU, US and Japan. Test protocols are available for single cell and fuel cell stacks testing; and Accelerated Stress Test (AST) and long-term steady state testing [Bloom et al., 2011; DOE, 2007; JRC-IE, 2010; USFCC, 2006; Volvo, 2004]. Some of the organizations that have contributed to these protocols are DOE and the US Fuel Cell Council (USFCC) in the US, Fuel Cell Testing and Standardization thematic Network (FCTESTNET) in the EU, and the FCTES^{QA} project, an international consortium (EU, Japan, US, etc.) to develop standardized fuel cell test procedures.

The main parameters that need to be controlled and monitored during fuel cell testing are, operating temperature, operating pressure, current density, cell voltage, reactants stoichiometry and consequently reactants flow rates. The system under investigation in the current work operates at atmospheric pressure and hence, no strict pressure control is required. The reliability of test results depends on how well all the above mentioned parameters are controlled and varied during test procedures. Another condition, which most of the characterization techniques that are mention in chapter 2, including the I-V curves and EIS require is, steady state condition to be ensured for measurements to be reliable.

It is with this in mind that all kinds of tests, including poisoning effects of impurities should be conducted. The poisoning effect of reformate impurities is a highly researched area in fuel cells, especially in PEM fuel cells, due to obvious difficulties related to obtaining and managing cost effectively pure hydrogen for fuel cell application [Andreasen et al., 2011; Büchi et al., 2009; Das et al., 2009; Yan et al., 2009; Zhang et al., 2006]. Consequently, hydrogen from the reforming of easily manageable liquid alcohols is usually preferred. The addition of reforming systems however, not only complicates the operation of a fuel cell system in general by adding auxiliary components such as the burner and the reformer, but also complicates the preparation of a comprehensive fuel cell test station. The reformate mixture contains gases such as CO that are poisonous to the Pt-electrocatalyst, and that could increase the chance for transient behavior during testing. This in turn can lead to less reliable and less reproducible results or to longer testing time.

Moreover, the reforming process does not normally go to a 100% conversion of reactants to the desired products, a fact which is rarely studied but can have effect on the performance and durability of a fuel cell. Therefore, it becomes even more complicated if the vapor constituents of reformate gas, i.e., methanol and water vapor in the case of methanol reforming are added to the impurities. Their addition calls for a separate vapor delivery systems, that has to be controlled together with the other stream of anode feed gases.

3.2 Preparation of the Test Station

For the experiments in the current work a complete single cell test station was built. As already mentioned the objective is to test the effects of the vapor constituents of the reformate mixture along with the gaseous impurities, and characterize the fuel cell's behavior under various conditions. To achieve this, a system that delivers the vapor mixture of methanol and water in a controlled manner is required. Two systems were tried, and the progress of the work is presented as follows.

3.2.1 First Setup: With a Bubbler System

Bubbler systems are very common, and their performances with respect to vapor-delivery precision depend on their application. A bubbler system is composed of a reservoir containing the liquid, whose vapor needs to be delivered and whose temperature is kept constant. A carrier gas is allowed to flow through this reservoir, and it takes the vapor up to where it needs to be delivered, which in the current case is the anode feed stream of the fuel cell. Vapor delivery systems can also work without a carrier gas, where, vapor flow in the outlet is either controlled by the vapor pressure of the liquid at a controlled temperature and then the flow in the outlet is manually restricted or simply by putting a mass flow controller in the outlet [Boer, 1995]. Many configurations were suggested to optimize bubbler systems and a number of patent claims have been made on controlled vapor delivery using bubbler systems [Lynch et al., 1986; Mcmenamin, 1983, 1984; Partus, 1980; Ross, 1977].

The reliability of a bubbler system for the purpose of delivering the vapor constituents of the refomate mixture in a controlled manner was tested. This is illustrated in fig. 3.1, where the bubbler, the mass flow controller for the carrier gas, the heating element, the temperature control and the fuel cell are shown. All components are controlled and monitored in a LabVIEW interface. The bubbler is controlled by controlling the temperature and carrier gas flow rate, in which the temperature of the liquid in the reservoir is measured and compared to the set–temperature and then the heating power is adjusted accordingly, so that the temperature in the reservoir is kept constant. This is a very crucial task for the proper functioning of the system, but at the same time very difficult to control, as it is not easy to account and compensate for all the heat transfers with only a heating element. Modeling details and assumptions made for the design of the bubbler system are reported in *paper 1*.

A mass flow controller, monitored and controlled in LabVIEW, delivers the desired amount of carrier gas. This gas, which is chosen to be CO_2 in this case but could have been H_2 or other inert gases as well, enters from the bottom of the reservoir and, by passing through the liquid, absorbs and carries up vapor. The vapor is then led to a stream of other gases, H_2 and CO, which are delivered by other mass flow controllers for a complete representation of a methanol reformate gas stream. Since the head space of the bubbler is assumed to be at atmospheric pressure condition, the LabVIEW control program controls the bubbler by only controlling the mass flow controller that releases the carrier gas necessary for the desired vapor delivery at a fixed temperature. Two measuring techniques were tried simultaneously for the vapor delivery, one in which a condenser was placed at the exit of the reservoir and another one where a transparent plastic tube was placed next to the reservoir to show the level of the liquid. The results had no real trend, and therefore, the comparison between the two and to the expected estimates was not possible. This confirms the fact that bubblers suffer from lack of reproducibility [Boer, 1995], and this is the case even for low flow rates, < 300 ml/min, which is the maximum limit for a linear relation between carrier gas flow

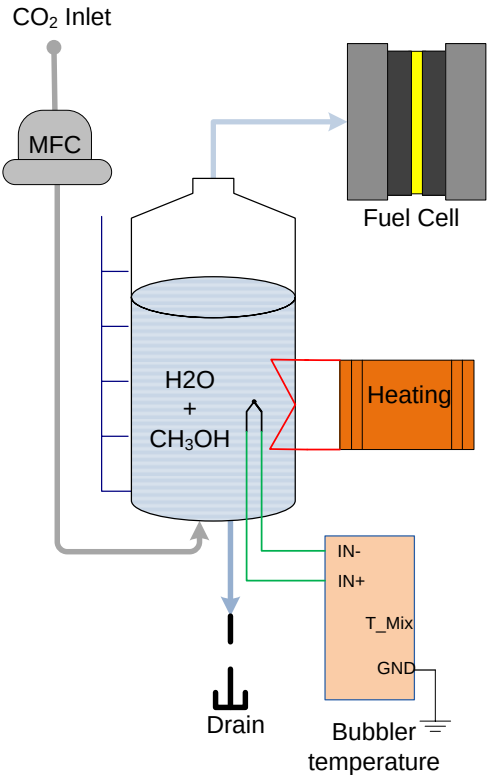

Figure 3.1: Bubbler system for vapor delivery.

rate and vapor carryover for isothermal conditions given by Love et al. [1993]. The reason for this could be that the assumptions made are too many, or perhaps the temperature control did not keep the liquid temperature within admissible fluctuation ranges. The fluctuation measured was less than 2 °C, and temperature being the main parameter causing irreproducibility, this shows how stringent temperature control is as a factor in bubbler systems.

The model could be validated by means of more sophisticated gas analyzers or mass spectrometers. However, this would nullify the advantage of a very cheap in-house preparation and control for which the bubbler system was considered at the first place. The scope was to achieve a cost effective, simple, and at the same time precise and reproducible vapor delivery for the range of typical flow rates of impurities in a unit cell assembly. The experiment showed that bubbler systems do not fulfill these requirements and therefore, another solution based on a dosing pump and an electrically heated evaporator was tested.

3.2.2 Second Setup: With an Evaporator System

As an alternative to bubblers for the delivery of methanol and water vapor in a simplified and precise way, a Grundfos DME dosing pump was tested. Downstream of the pump is placed an electrically heated evaporator that boils all the mixture of liquids or the pure liquid passing through it. The pump is a self-priming diaphragm pump and both the pumps suction strokes and the heating of the evaporator are controlled in LabVIEW. Figure 3.2 illustrates the concept with all the components involved. The dosing pump, pumps the liquid mixture from the reservoir to the evaporator, which is kept at constant temperature, well above the boiling point of either of the liquids, at around 150 °C. The vapor is then directed to the anode inlet along with a stream of the other gases composing the reformate gas, H_2, CO_2 and CO. The flow rates of these gases are controlled by appropriate mass flow controllers.

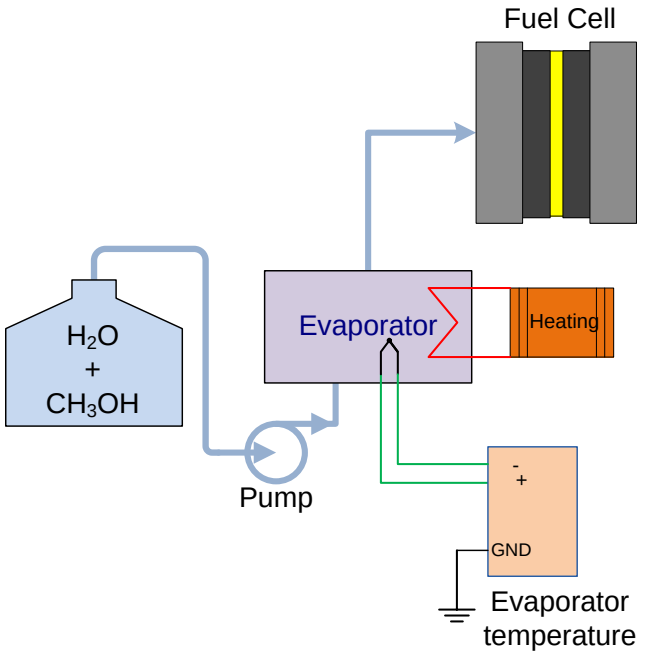

Figure 3.2: Evaporator system for vapor delivery.

A mixture of water and methanol does not form an azeotrope, meaning that there is no composition ratio, in which the boiling point of the solution is higher or lower than either of the pure liquids. This allows validation experiments to be carried out with water alone and conclusions to be drawn for the mixture. This is possible because the boiling point of the solution, at any composition, lies in the

temperature range between 64.6 °C - 100 °C, which are boiling points of methanol and water at atmospheric pressure, respectively. Therefore, tests were performed with water alone and they showed that with a pump that allows such small liquid flow rates there is satisfactory vapor carryover. There is though a very little risk of condensation when the flow rates and the distance to the fuel cell increase.

The heating power needed to boil the liquid flowing through the evaporator can be calculated by Eqn. (3.1)

$$P = q\rho\left(c\Delta T + L_v\right) \tag{3.1}$$

where P is the required heating power [kW], q is the liquid flow rate [m^3/s], ρ is the density of liquid [kg/m^3], c is the specific heat capacity of liquid [kJ/kgK], ΔT is the temperature difference between the reservoir and the evaporator [K] and L_v is latent heat of vaporization [kJ/kg].

As in the case of the bubbler system, the temperature of the evaporator is continuously monitored and the heating power is regulated by comparing the measured temperature with the temperature set in LabVIEW. This way temperature is kept constant and a continuous flow of vapor is ensured. Unlike in the case of the bubbler system, here temperature control is not so crucial, as far as it is set high above the boiling point of water.

Table 3.1: Observation on the performance of the evaporator system

Liquid flow rates [ml/min]	**Application**	**Vapor carryover**
0.025-0.05	- Unit cell testing at low stoichiometry	- No condensation
0.08-0.5	- Unit cell at high stoichiometry and small stacks testing	- No condensation
≥ 3	- Fuel cell stack testing	- Condensate formation

The volume flow rate of methanol-water mixture was taken to be 10 % of the total anode feed gas. This corresponds to $0.025\,\mathrm{ml/min}$ in liquid phase, for the unit cell assembly of total active cell area of 45 cm^2, operating at H_2 stoichiometry(λ_{H_2}) of 1.2, air stoichiometry (λ_{air}) of 4 and current of 15 A. Tests were performed for liquid flow rates up to $0.05\,\mathrm{ml/min}$, for eventual operation of the same unit cell assembly at higher fuel cell current densities. It was observed that all the liquid boiled and was carried away as vapor. However, special attention need be paid on the length and insulation of tubes that take the vapor from the evaporator to the fuel cell, since temperature drop at the exit from the evaporator may cause condensation. The length of the tubes needs to be minimized and they need to be well insulated or even heated, as the condensate may enter a non-operating fuel cell and leach the acid doping of the PBI membrane. This is however facilitated by the fact that the temperatures of the evaporator and an operating HT-PEMFC

are very similar, and the two can be places as close to each other as possible and thereby avoid heat loss between them.

Medium flow rates between $0.08\,\mathrm{ml/min}$ and $0.5\,\mathrm{ml/min}$ were also tested and results showed that there is good vapor carryover in this range as well. This makes such vapor delivery system a suitable candidate, not only for a unit cell testing at higher current densities and higher stoichiometric ratios but also for small fuel cell stacks testing. Finally, tests were done for liquid flow rates of above $3\,\mathrm{ml/min}$, where a slow temperature drop down to below the boiling point of water was registered. This temperature would then remain constant at a couple of degrees Celsius below the boiling point of water and cause the dripping of water droplets along with the vapor. However, these flow rates are way above the typical liquid mixture flow rates necessary for single cell tests, and hence the use of the evaporator system is suitable enough for the study of the effects of methanol and water vapor slips in H_3PO_4/PBI–based HT-PEMFC unit cell assembly. Vapor carryover without condensation maybe achieved even for high flow rates by increasing the size of the evaporator and the heating power supplied. The observations are summarized in Tab. 3.1.

3.2.3 Final Setup

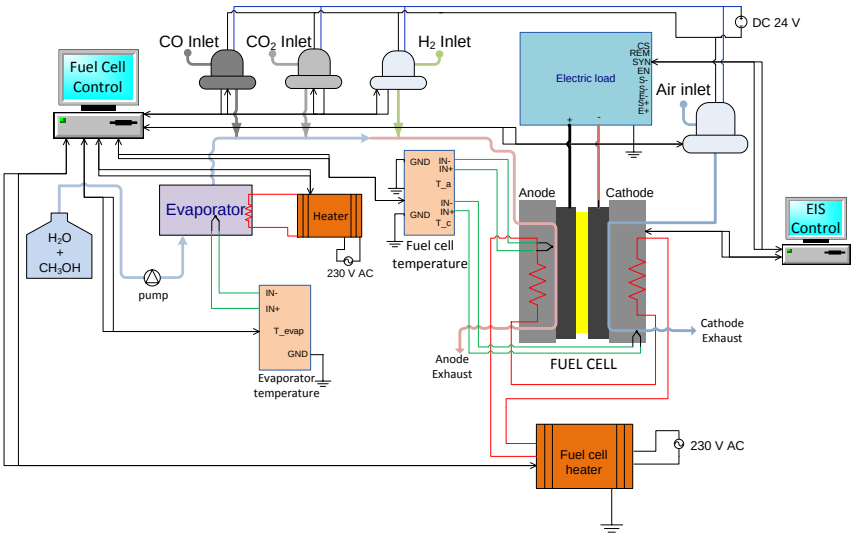

Figure 3.3: HT-PEMFC unit cell test set-up comprising an evaporator system for vapor delivery and fuel cell control and EIS data acquisition system.

Based on the studies above a vapor delivery by means of an evaporator system was found to be more reliable for the purposes the current research project. There-

fore, it was chosen for inclusion in the final test station for a complete and controlled simulation of reformate mixture. For better precision a pump with lower limits was employed in the final test set-up. The complete test station is illustrated in Fig. 3.3 and a photo of the main components is given in Fig. 3.4. The fuel cell used is a unit cell assembly of a 45 cm^2 active area with a Celtec® P MEAs from BASF, sandwiched between graphite composite flow plates of serpentine flow channels.

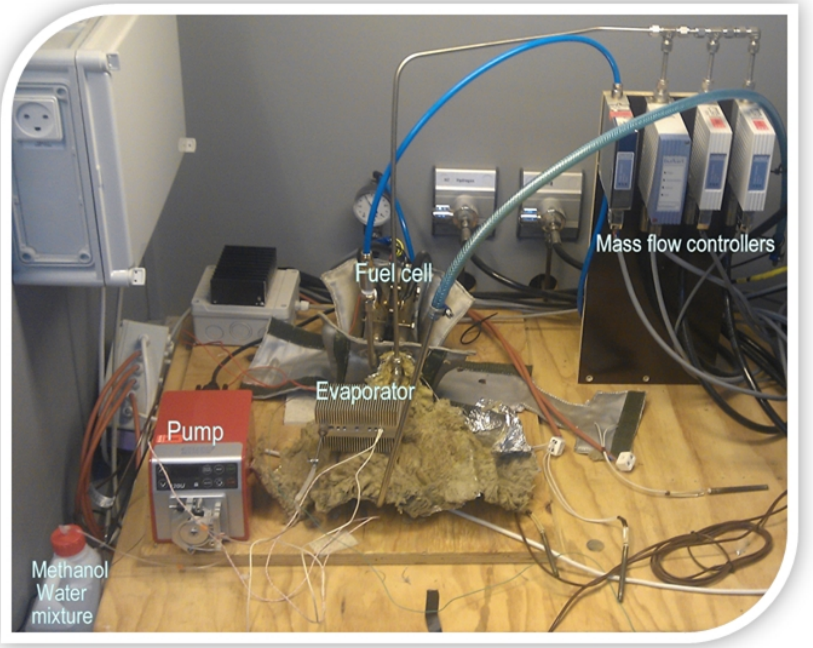

Figure 3.4: Photo of the HT-PEMFC unit cell test set-up.

The system is controlled and monitored entirely in a LabView interface. Hence, data acquisition systems from national instruments are used for signal processing and control of the operation of the fuel cell system by controlling flows through the mass flow controllers for the gaseous constituents, the fuel cell temperature and the evaporator temperature.

EIS, whose use is previously described in this dissertation, is the tool of choice for characterization in the current work. Despite some of its limitation, if performed carefully is a strong tool that can give a variety of qualitative insights into changes within a fuel cell. Some of the limitations are, the risk of non-linearity if the the induced AC amplitude is not small enough, and the fact that multiple EC models can fit the same data. In this project two impedance measurement systems are tried, an in-house developed LabView based measurement system and

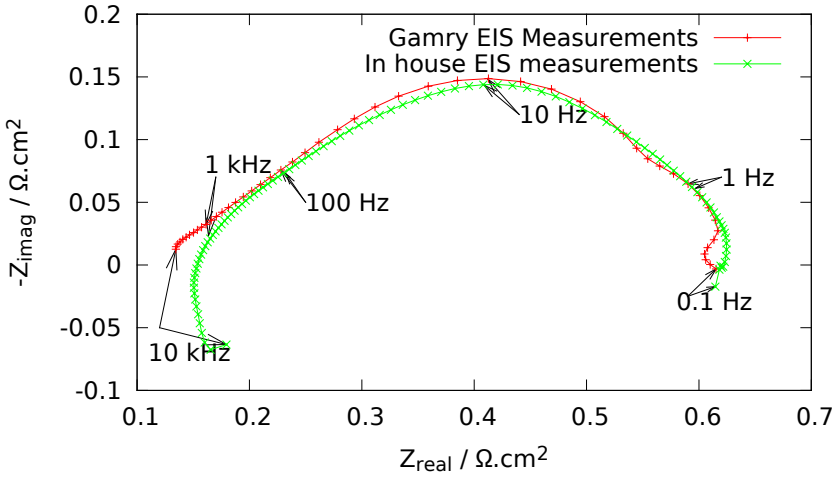

Figure 3.5: Comparison of two impedance measurement systems at 120 °C and 10 A, a commercial one from Gamry and an in house prepared measurement system.

another system acquired from Gamry, FC350^{TM}. Measurements taken by the two systems are compared to each other in Fig. 3.5, and as can be seen except for small discrepancies in the two ends of the frequency sweeps the measurements are in agreement with each other. The Gamry impedance measurement system was used for majority of the tests in this work.

Data analysis was done by fitting measured impedance data to EC models. Equivalent circuit modeling was done by attempts based on the knowledge of the fuel cell and the number of time constants observed in the impedance spectra. Once the EC model is chosen measured data is fitted to the EC model by means of a fitting software, ZView^{TM} (Scribner Associates, Inc.). The software employs Complex Non-linear Least-Square (CNLS) method for fitting and error estimation, and then the resistances of the different ranges of frequency sweep are analyzed.

Summary

In this chapter, a complete single cell test station capable of testing various operating conditions and fuel compositions was presented. A vapor delivery system is necessary for a comprehensive testing of all the constituents of a methanol–based reformate, and was included in the test station. A bubbler system was found to be inappropriate for such application due to lack of reproducibility, even for small flow rates such as those involved in the operation of a unit cell assembly. An evaporator system, on the other hand, was found to be reliable for the purposes of the current work.

The following chapters are the analysis and interpretation of the various characterization tests performed on a H_3PO_4/PBI–based HT-PEMFC. The above described single cell test station was used for all the experimental work.

4 Results and Discussion

In this section the main contributions of the current research project are given, in relation to the available literature and the stated objectives. Statements on the effects of impurities on the performance of an HT-PEMFC are given based on the analyses of data acquired during the experiments. An attempt made to qualitatively relate the combined effects of impurities with individual effects is also presented.

4.1 Background

The characterizations reported here are results already disseminated in various forms as mentioned in the list of papers given on page VII. For ease of reading, effects of impurities are characterized individually first and then in relation to each other. For this, results from the different tests and publications are put together for an overall analysis. In *paper 4*, the effects of the gaseous impurities, CO and CO_2 are given at different operating conditions. In *paper 3*, the effects of vapor constituents of reformate mixture; methanol and water are analysed as a mixture. Then, in *paper 2* the combined effects of all impurities are analysed and a preliminary interdependence study among the impurities is provided. The chronological order in which the tests for the different characterizations were performed do not coincide with the numbering given to the papers, in fact, *paper 4* is the earliest study of all, followed by *paper 2* and then *paper 3*.

Degradation in this work is defined as the loss in fuel cell performance due to impurities, other non-ideal conditions and aging. Performance losses can be either reversible as in the case of CO poisoning or irreversible as in the case of peroxy radical attacks, membrane thinning, loss of ECSA and other mechanical failures

[de Bruijn et al., 2008; Kundu et al., 2008]. Reversible performance losses can be recovered by either simply ending introduction of the impurity or by performing a recovery procedure [Borup et al., 2007]. Irreversible losses on the other hand are permanent and usually cause failure of the MEA, and therefore, of the fuel cell.

The performance losses in this work are mainly caused by catalytic degradation, surface adsorption of impurities on Pt surface or by means of Pt sintering, both manifested as losses of ECSA; or by membrane degradation, mainly phosphoric acid leaching and other unidentified mechanisms that can be caused by methanol–water vapor mixture. Therefore, it is difficult to distinguish between reversible and irreversible performance losses without performing recovery procedures, even in that case some of the losses can be only partially reversible. Therefore, in this work, recovery test was performed after a durability test, in the presence of methanol-water vapor mixture, to check the reversibility of the effects.

4.2 Effects of CO

4.2.1 Mechanisms of CO Poisoning

The sensitivity to CO of PEMFCs is one of the main concerns that surround the issue of their reliability. This has led over the years to an extensive study of characterization of the effects of CO both in LT-PEMFCs and HT-PEMFCs [Andreasen et al., 2011; Büchi et al., 2009; Das et al., 2009; Du et al., 2009; Yan et al., 2009; Zhang et al., 2006]. The main reason to this attention on the effects of CO is its inevitable presence in the outcome of a reforming process, and the cost and complexity of purification techniques. While there is a general agreement on the mechanisms by which it attacks the catalyst of a PEMFC, there still remains a margin for better and more definitive explanation of its effects. The Pt electrocatalyst is the most sensitive part of the fuel cell to this contaminant, by means of preferential adsorption on the Pt surface and consequent Pt-CO formation, which is more exothermic than Pt-H formation [Du et al., 2009]. CO adsorption mode on Pt surface is reported to be mainly a linear bond, and its effect on the fuel cell current density (i), and therefore on the fuel cell performance has been modeled according to Eqn. 4.1 [Li et al., 2003; Song et al., 2008],

$$\frac{i_{\mathrm{H_2+CO}}}{i_{\mathrm{H_2}}} = (1-\theta_{\mathrm{CO}})^2, \tag{4.1}$$

where, $i_{\mathrm{H_2+CO}}$ and $i_{\mathrm{H_2}}$ are the H_2 oxidation current densities with and without CO, respectively, and θ_{CO} is the Pt surface coverage of CO. Under conditions more appropriate to the operation of PEMFCs, Eqn. 4.1 is reduced to Eqn. 4.2 [Li et al., 2003],

$$\frac{i_{\mathrm{H_2+CO}}}{i_{\mathrm{H_2}}} = (1-\theta_{\mathrm{CO}}). \tag{4.2}$$

The physical meaning of the current ratio in Eqn. 4.2 is the relative activity of the catalysts for hydrogen oxidation in the presence of CO, where value one of the ratio indicates no change in the number of active catalyst surface sites for the hydrogen oxidation even in the presence of CO [Li et al., 2003]. In either one of the relations above increasing θ_{CO} decreases i_{H_2+CO}, i.e., the H_2 oxidation current density decreases, meaning that the performance decreases, as the CO surface coverage θ_{CO} increases.

4.2.2 Temperature and Tolerance to CO Poisoning

The fundamental understanding of the poisoning mechanism of CO, both by means of modeling and experimental studies has led to a number of proposed mitigation methods. Some methods regard the reforming process, where the CO content is reduced by means of Water Gas Shift (WGS), Preferential Oxidation (PROX), membrane separation, or methanation [Li et al., 2003]. Other methods involve the fuel cell itself, in which the operation conditions are changed or more tolerant materials are used. Operating the fuel cell at higher temperature increases its tolerance to CO poisoning. However, for the tolerance to be acceptable with regards to the amount of trace CO in reformate gas, without any pre-treatment, the fuel cell should be operated at significantly higher temperatures than 100 °C. Hence, the HT-PEMFC, a whole new fuel cell type which other than operating at different temperature conditions also uses a different acid-based polymer membrane with respect to its low temperature counterpart was invented.

The dependence of CO poisoning on the operating temperature of a Pt-based PEMFC can be analytically modeled as follows [Song et al., 2008];

$$\theta_{CO} = \frac{-\Delta G^0}{r} - \frac{RT}{r} lnH + \frac{RT}{r} ln[CO]/[H_2], \tag{4.3}$$

where ΔG^0 is the standard free energy of adsorption, r is the interaction parameter, H is the Henry's law constant for CO solubility, [CO] and [H_2] are concentrations of CO and H_2 respectively.

Experimental results confirm the advantages of higher temperature operation as shown in Fig. 4.1. The figure shows a Nyquist plot of a single cell running on H_2 and 0.5% CO at 9 A (0.2 A/cm^2) and varying temperature from 120 °Cto 180 °C. It is evident from the plot that fuel cell impedance increases with decreasing temperature. At 120 °Cthe impedance spectrum is much larger than the other spectra at higher temperatures, especially in the intermediate frequency range. This indicates that anode poisoning effects have a potentially devastating effect on the intermediate frequency impedance. The increase of the intermediate frequency arc agrees with results obtained by Jiang et al. [2005], from studies of Nafion®– based PEM fuel cells operated above 100 °C. They suggested that the observed increase in impedance was due to the decrease in Relative Humidity (RH) while increasing the temperature from 105 °C–120 °C. This means that there is lower water vapor content for electrochemical oxidation of adsorbed CO to take place. This negative

effect over weighs the benefit of the suppression of CO adsorption obtained by increasing the temperature in that temperature range.

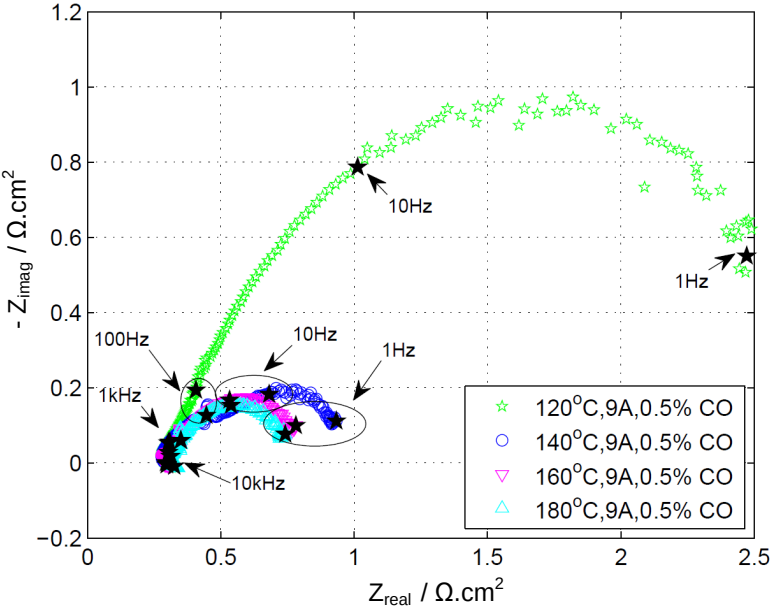

Figure 4.1: Nyquist plot of a single cell running on H_2 and 0.5% CO at 9 A (0.2 A/cm^2) and varying temperatures from 120 °C to 180 °C.

4.2.3 CO Poisoning in Relation to other Non-ideal Conditions

In *paper 2*, where the effects of all methanol reformate impurities were tested, the effects of CO in relation to other impurities were analyzed. 1% and 2% CO were tested and in line with the literature on CO poisoning it was found that CO has the most severe degrading effects compared to the other constituents of a reformate gas. Consequently, its addition to the anode feed causes the degradation in the fuel cell performance immediately. As a manifestation of the fact that the poisoning affects mainly the catalyst layer, the increase in resistance due to CO poisoning is most pronounced in the high frequency region of the measured impedance spectra. It adsorbs on the active Pt sites of the electrodes, both anode and cathode (maybe through CO crossover) and slows the respective half-cell reactions, without affecting so much the proton conductivity of the electrolyte. The effect of CO poisoning on both anode and cathode is also reported in [Cheng et al., 2007].

4.3 Effects of CO_2

Another byproduct of the reforming process is CO_2, usually present up to 25% by volume in the anode feed gas. Similarly to the effects of CO, most of the changes are seen in the high frequency region. This implies that the effects are concentrated on the catalyst layer here as well. In fact, the effects of CO_2 can be redirected to those of CO, as it can be reduced to CO through either Reverse Water Gas Shift (RWGS), Eqn. 4.4 or directly in the cathode according Eqn. 4.5 [Du et al., 2009];

$$CO_2 + H_2 \longleftrightarrow CO + H_2O. \tag{4.4}$$

$$CO_2 + 2\,H^+ + 2\,e^- \longrightarrow CO + H_2O. \tag{4.5}$$

4.3.1 Temperature and CO_2

In the tests in *paper 4*, in agreement with the general notion, no significant changes are seen in any of the frequency ranges at 180 °C. At lower temperatures however, some losses in performance are observed as can be seen in the increase in high frequency resistance in Fig. 4.2. The explanation may reside in the fact that CO_2 is not completely inert, but loosely binds to Pt-surface, and may be reduced to CO [Du et al., 2009].

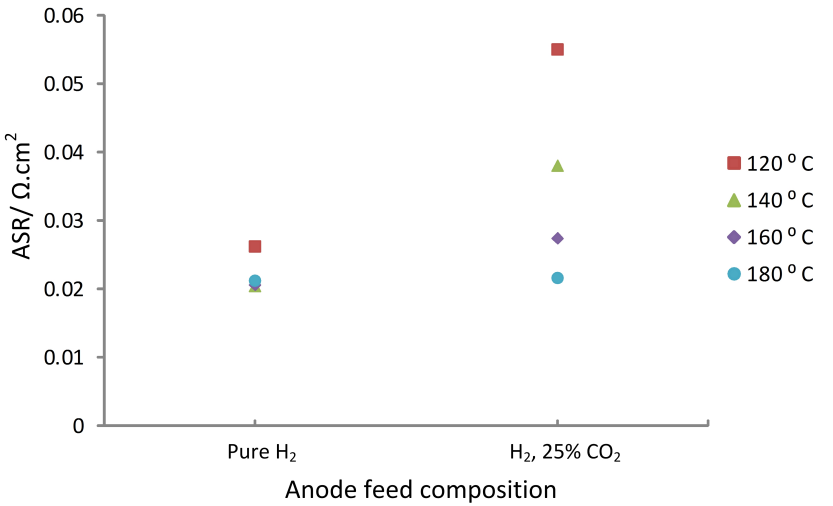

Figure 4.2: High frequnecy resistance in the presence of CO_2 at 0.2 A/cm^2 and varying temperature from 120 °C to 180 °C.

It is reported that in the case of LT-PEMFCs poisoning effects of CO_2 increase with the increase in temperature as the kinetics of the RWGS increase to produce

more CO [de Bruijn et al., 2002]. This is not seen in HT-PEMFCs, possibly because the negative effects of the increase in RWGS kinetics are counteracted by the decrease in preferential CO adsorption and removal by electrooxidation of adsorbed species at higher temperatures. Another explanation could be that, owing to the faster diffusion of reactant gases, the dilution effects of CO_2 are lower at higher operating temperatures.

4.3.2 CO_2 and Current Density

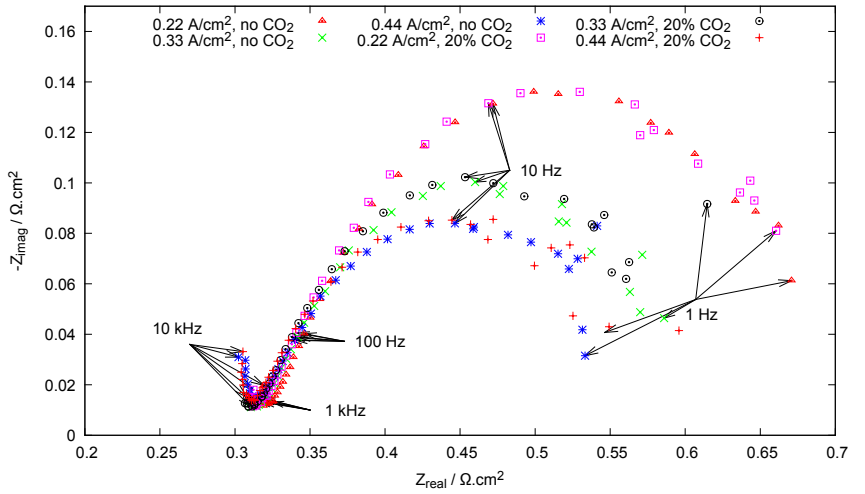

Figure 4.3: The effect of 20% CO_2 at varying current density on a PBI–based HT-PEMFC operating at 160 °C.

In another test in *paper 2*, where the effects of all impurities were tested the effects of CO_2 were found to be negligible at varying current density. Figure 4.3 shows that the impedance spectra overlap for almost all the measured current densities both in the case of pure H_2 gas and when 20% of the anode feed is CO_2. The only exception is seen at 0.22 A/cm^2, where the high frequency semi-circle is slightly shifted to the left in the presence of 20% CO_2, while the low frequency one remains unaltered. This shows that while as already seen CO_2 exacerbates the effects of CO, it does not have significant effect on the losses of a fuel cell, if tested alone, especially in this case where the stoichiometric ratios are relatively high, 1.2 for hydrogen and 4 for air.

4.4 Effects of Methanol-Water Vapor Mixture

The effects of methanol-water vapor mixture are tested both along with all the impurities (in *paper 2*) and alone (in *paper 3*). In both studies, temperature was kept constant at 160 °C, and for the methanol-water vapor mixture, a steam to carbon ratio of 1 is considered throughout the duration of the experiments.

The increase in vapor mixture concentration causes resistances to increase as in the case of CO and CO_2, with minimal increase for 5% vapor mixture by volume in feed gas. More significant performance degradation is observed when the vapor mixture is increased to 10%. Like with CO, the changes are slightly more pronounced for high frequency range, signifying here also that the catalyst kinetics is affected the most. The mechanism by which it affects the could be by means of methanol dehydrogenation process which is known to happen on Pt surface according to the reaction in Eqn. 4.6 [Sriramulu et al., 1999],

$$\mathrm{CH_3OH + Pt \longrightarrow Pt{-}CO + 4\,H^+ + 4\,e^-}. \tag{4.6}$$

This produces CO_{ads}, which as mentioned previously has a poisoning effects on the Pt catalyst by preferential adsorption. Moreover, the surface coverage by CO_{ads} can also impede CO oxidation [Modestov et al., 2012], which is a way of CO removal from the Pt surface.

PBI membrane that is employed in the tested fuel cells is also reported to permeate methanol, mainly by diffusion. In fact, methanol permeation through polymer membrane with subsequent dehydrogenation on the catalyst is one of the main degradation concerns in DMFCs. Moreover, the dehydrogenation process has complex non–CO intermediates at certain potentials, such as formaldehyde and formic acid [Cao et al., 2005; Iwasita, 2002], which could have undesired effects on the operation of a fuel cell.

As reported in *paper 3*, a durability test was performed over a period of 1250 hours in the presence of methanol-water vapor mixture in the anode feed gas at different concentrations. The voltage drop was continuously registered, and EIS measurements were taken for the entire period of tests and analyzed by fitting to an EC model. At the end of the impedance tests, the fuel cell was disassembled and SEM was performed on the MEA and compared to an unused MEA of the same type. PA levels and Pt- distributions were also measured along the cross-section for comparison with a new MEA.

4.4.1 Analysis of Voltage Drop

In Fig. 4.4 the voltage drop of the fuel cell is given in voltage-time plane for the entire period of tests. It is observed that the degradation rate for operation on pure hydrogen taken over a period of 123 hours gives a near horizontal line, with an average drop rate of -5 μV/h. Schmidt and Baurmeister [2008] also found the same voltage drop of -5 μV/h over a period of 3000 and 6000 hours, respectively, for the same MEA type. Their tests were long-term durability studies on HT-PEMFC at

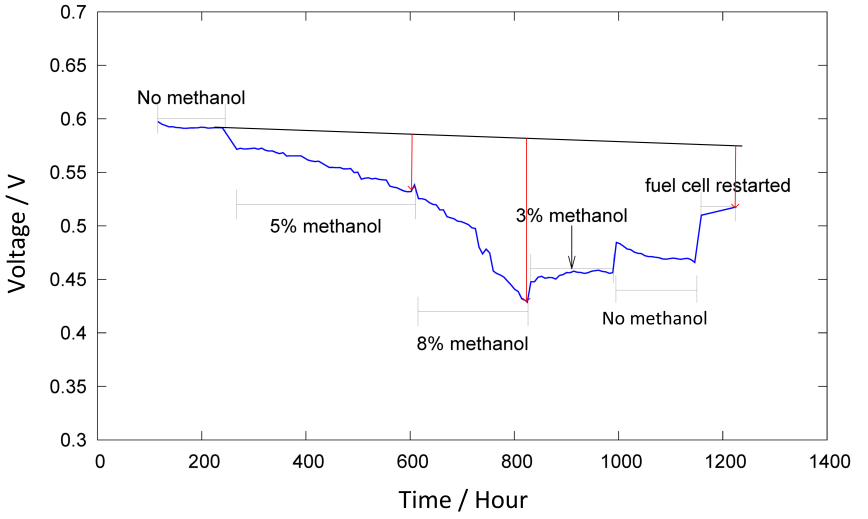

Figure 4.4: Cell voltage during the entire period of experiments in the presence of methanol-water vapor mixture for a fuel cell operating at 0.22 A/cm^2 and 160 °C. The red arrows pointing down, show the voltage drop at relevant test points, where the methanol content was changed

cell temperature of 160 °Cand current density of 0.2 A/cm^2. This is in agreement with the degradation rate claimed by BASF for the MEA. Moçotéguy et al. [2009] found a higher voltage drop rate of -41 μV/h over a period of 505 hours on a Celtec-P1000 MEA, at a higher current density of 0.4 A/cm^2 and temperature of 160 °C.

In comparison, operation in the presence of 5% by volume of methanol-water vapor mixture in the anode feed gas shows a degradation rate of -900 μV/h, which is evidently deviated from the case of a pure hydrogen operation. Li et al. [2009] worked with reformate in their long-term durability tests with a voltage drop rate of -20 μV/h, which however cannot be directly compared with the current work as they used natural gas reformate.

Further increase in methanol content to 8% produces even steeper degradation slope. The rate in this case is -3.4 mV/h and degradation continued without any sign of stabilization until the methanol content in the feed gas was reduced. The concentration was reduced to 3% by volume and this caused a rapid recovery in the beginning, which then continued slowly until the supply was shut down. The total recovery was a modest 0.03 V over 157 hours with respect to a total voltage drop of 0.17 V, caused by the vapor mixture until that point over a period of 988 hours. When the methanol supply was interrupted, further recovery of the performance of the fuel cell followed by slow degradation was observed. The degradation rate on pure hydrogen of the aged fuel cell after tests with vapor

mixture was faster than the rate before tests with vapor mixture had been started. However, the initial recovery due to the interruption was high enough to keep the cell voltage above the levels of operation on 3% vapor mixture concentration as can be seen in Fig. 4.4. The fuel cell was restarted before end of tests and a significant rise in voltage was noticed, 11% increase in cell voltage.

4.4.2 Analysis of Impedance Spectra

In Fig. 4.5 it can be seen from the Nyquist plot that the impedance spectra expands with time and with the introduction of the methanol-water vapor mixture, while also being displaced to the right on the real axis. The bode diagram also shows that the maximum phase shift and the frequency at which it occurs increases with time. Similar trend of expanding spectra is seen in [Mamlouk and Scott, 2011] with decrease in temperature of a HT-PEMFC, and is a typical indication of increased losses manifested by increased impedance.

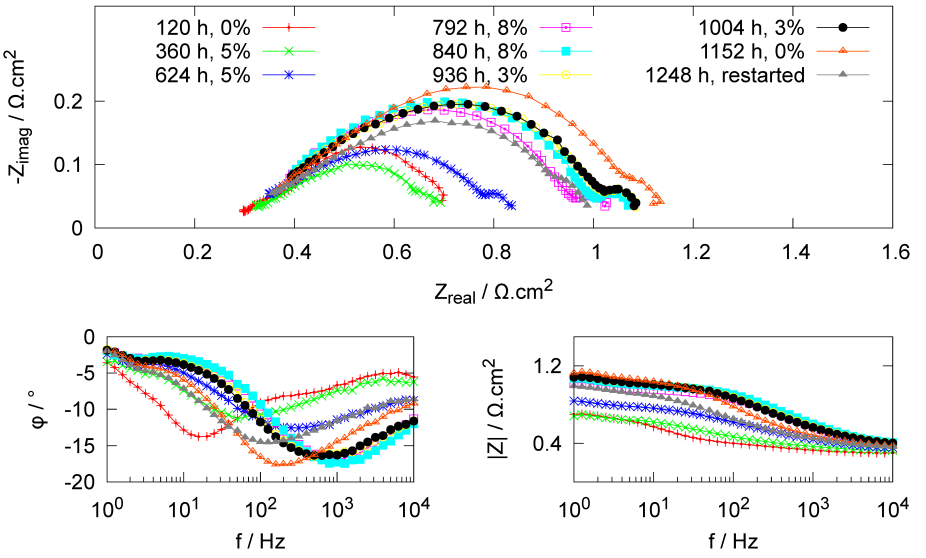

Figure 4.5: Impedance spectra and bode plots showing the effects of different concentrations of methanol-water vapor mixture in the anode feed gas.

Contrary to expectations, the spectra in Fig. 4.5 do not show any inductive behavior at high frequency. High frequency inductive behavior is usually present in impedance measurements due to the wiring and other instrumental non-idealities [Andreasen et al., 2011; Mamlouk and Scott, 2011]. In the current work the recommended wiring supplied by Gamry was used to connect the impedance measurement system to the fuel cell, and other wires were used for the rest of the setup.

Mamlouk and Scott [2011] limit the inductive behavior to above 10 kHz. Otomo et al. [2004] on the other hand did not see a high frequency inductive behavior in their sweep of until more than 10 kHz, but observed instead, a low frequency inductive loop for methanol electro-oxidation in the anode. Despite these uncertainties and relatively high $-Z_{imag}$ values, the changes in impedance observed due to variation in the concentration of methanol-water vapor mixture are rather typical of performance degradation, and follow closely the overall durability plot in Fig. 4.4. It can also be noticed that, a high frequency loop is only seen on measurements before the tests with methanol started, after which instead a low frequency semicircle evolves increasingly with time and with increase in methanol concentration. Moçotéguy et al. [2009] also observed that the high frequency loop disappears with increase in degradation, which makes it plausible to suggest that the disappearance of this loop is related to increased degradation from poisoning due to methanol.

In the beginning, as methanol-water vapor mixture was introduced to the system the impedance spectrum shrinks, as can be seen in Fig. 4.5. This shrinking of spectrum could imply that the vapor mixture has an initial positive impact on performance. This may be attributable to the presence of water vapor, which enhances the cell performance by promoting the proton conduction through the membrane [Daletou et al., 2009]. However, water is also reported to have a degrading effect by leaching the H_3PO_4 from the PBI membrane at lower temperatures during fuel cell shut down [Liu et al., 2006]. This is expected to be limited in the current work, as there were no start/stop cycles tested, in which dilution of acid at lower temperature during shut down is suggested [Gu et al., 2010].

Further continuous operation at 5% and then successively at 8% causes the impedance spectra to continuously expand. This expansion implies loss in cell performance with time, according to the increase in methanol concentration. The increase in spectra size stops for operation at 3% of vapor mixture, suggesting that poisoning effects are only seen at high concentrations of vapor mixture. When the vapor supply is interrupted a sudden recovery followed by slow degradation in performance was observed. This could mean that a small amount of vapor mixture may enhance the performance by humidification, which is also seen when methanol was first introduced to the fuel cell.

At the same time, it is observed that more methanol in anode feed means more pronounced low frequency loops. In fact, the shapes of the spectra before methanol was introduced and after methanol supply was interrupted resemble each other in the low frequency region, in that, they have less pronounced low frequency loops. Otomo et al. [2004] observed an inductive loop at frequencies lower than 0.1 Hz. They concluded that since the inductive loop appeared through the electro-oxidation, it was an indication of the fact that during the electro-oxidation of methanol the passage from the intermediates to the products was the rate-determining process of the overall reaction. The low frequency loop in this case could be characterized by the start of such behavior, or just mass transport and diffusive limitations. In either case it can be said that, methanol-water vapor mix-

ture increases the losses in this frequency range. Ji et al. [2008] reported that the hydroxyl groups of methanol forming hydrogen bonds, are more likely to accept hydrogen atoms than to donate hydrogen atoms. This may slow down diffusion of hydrogen in the anode side, implying that diffusion losses are not limited to the cathode side alone.

4.4.3 Analysis of Fitted Resistances

The impedance spectra in Fig. 4.5 are fitted to an EC model shown in Fig. 4.6. The fitted results of the resistances at the different frequency regions are given in Fig. 4.7, and analyzed thereafter.

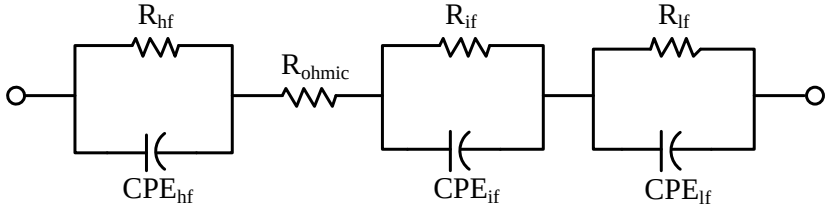

Figure 4.6: Equivalent circuit model fitted to experimental impedance measurements for data analysis.

Ohmic Resistance (R_{ohmic})

Generally speaking, there is not significant change in ohmic resistance. There is a slight decrease in R_{ohmic} at all the stages of the tests, but it is cancelled out by the increase seen at each change of methanol content in feed gas. Assuming that, R_{ohmic} represents the contact resistances and electrolyte resistance, it can be said methanol-water vapor mixture has negligible effect on the overall conductivity of the electrolyte. The slight decrease in R_{ohmic} observed in all the stages of the tests, may be attributed to the presence of water vapor, which enhances the proton conduction in PBI–based polymer electrolytes [Daletou et al., 2009].

On the contrary, the same reasoning done earlier on the H_3PO_4 leaching effect of vapor mixture at lower temperatures can be done [Liu et al., 2006]. Moçotéguy et al. [2009] observed H_3PO_4 leaching without significant changes in R_{ohmic} in their long-term durability tests that included start/stop cycling.

High Frequency Resistance (R_{hf})

There is a clear increase in R_{hf} in the presence of 5% methanol as can be seen in Fig.4.7. The increase is strangely arrested when the methanol content is raised

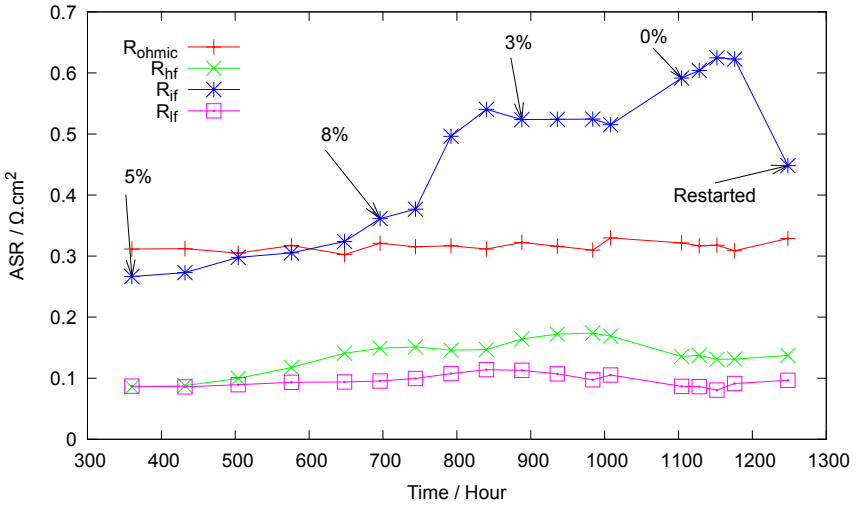

Figure 4.7: Cell voltage during the entire period of experiments in the presence of methanol-water vapor mixture.

to 8%, and then slightly increases on the passage to and during operation at 3%, where it then remains constant towards the end. Lastly, when methanol-water vapor supply was interrupted the effects reversed partially and remained constant even after the fuel cell was restarted.

Thus, it appears that, it is more the change in vapor content of the feed gas that determines the magnitude of R_{hf} than the vapor content itself. This is seen from the fact that R_{hf} increases every time the amount of vapor is changed, and then stabilizes. A possible explanation for this could be that, some saturation or equilibrium condition is established at the interface after each change in concentration.

Intermediate Frequency Resistance (R_{if})

In the intermediate frequency range, a slow and progressive increase in resistance is seen during operation with 5% methanol. The increase is then more pronounced for 8% and continues to increase until the methanol content is reduced to 3%, where R_{if} remains constant. It is as if operation on 3% methanol by volume stops the increase in R_{if}, which resumes when methanol supply is interrupted.

It is also interesting to notice that, R_{if} follows closely the trend of the durability profile in Fig. 4.4, and therefore, can be a useful parameter for fuel cell diagnosis. That is, the increase in R_{if} corresponds to increased voltage drop due to catalyst degradation and can be a good indication of the state of health of the fuel cell.

Although, the intermediate frequency region is usually associated with charge transfer limitation of cathodic Oxygen Reduction Reaction (ORR) [Zhang et al.,

2009], some processes in the anode side may also contribute to part of these resistances. It also seems that, some of the degradations due to methanol-water vapor mixture are reversible, from which the fuel cell recovered fast when restarted.

Low Frequency Resistance (R_{lf})

Similarly to the R_{if}, the R_{lf} also showed a successive increase for 5% and 8% methanol-water vapor mixture, proportionally to the vapor content. Unlike in the former case however, an initial decrease followed by slight increase was observed both during operation with 3% vapor mixture and when the supply of vapor was interrupted. The low frequency loop is usually characterized by diffusion limitations in the GDL [Gomadam and Weidner, 2005], which may results in the same limitations on the catalyst surface as well. This could imply, that higher contents of vapor mixture increases these diffusion losses, while small amount of vapor may promote the diffusion of the gaseous species both on the GDL and the catalyst layer.

4.4.4 Post-Mortem Analysis

A visual idea of the degradation of the MEA can be seen from the differences in the SEM images in Fig. 4.8 and the atomic distributions in Fig. 4.9. It should be noted that the two images were taken at different scales, the new one at a scale of 30 μm and the used one at 100 μm. Nonetheless, the degradation caused during the operation of the fuel cell can be noticed from the less uniform distribution of the Pt particles (white area) in the used MEA.

The peaks in the atomic distributions are displaced, possibly due to the swelling caused by the intake of the different species in the anode feed, which may also have caused increased thickness of MEA as can be noticed both in Fig. 4.8 and in Fig. 4.9. This is in contrast with Liu et al. [2006], where a slight reduction in membrane thickness is seen after a degradation test. This could be due to the presence of condensed methanol and water in the MEA. It could also be that the membrane has lost the compression it was subjected to during tests before the SEM images were taken, and this relaxation combined with the intake of methanol and water molecules could have caused the swelling. The PA and Pt counts are also more on the used MEA than the new one. This is mainly because different MEAs are not identical to each other, and even within the same MEA different cross-sections may have different levels of Pt and PA.

Contrary to expectations, the visible increase in membrane thickness did not cause visible decrease in the proton conductivity of the PBI–based electrolyte. This can be suggested from the fact that, despite the increase in the thickness of membrane, R_{ohmic} does not change much throughout the tests. This may be due to some counter acting effects, where the presence of water vapor enhances the membrane conductivity and the membrane thickening inhibits it.

A slightly higher concentration of Pt is seen on some points of the cathode side of the used MEA with respect to the unused one. This could be Pt particle

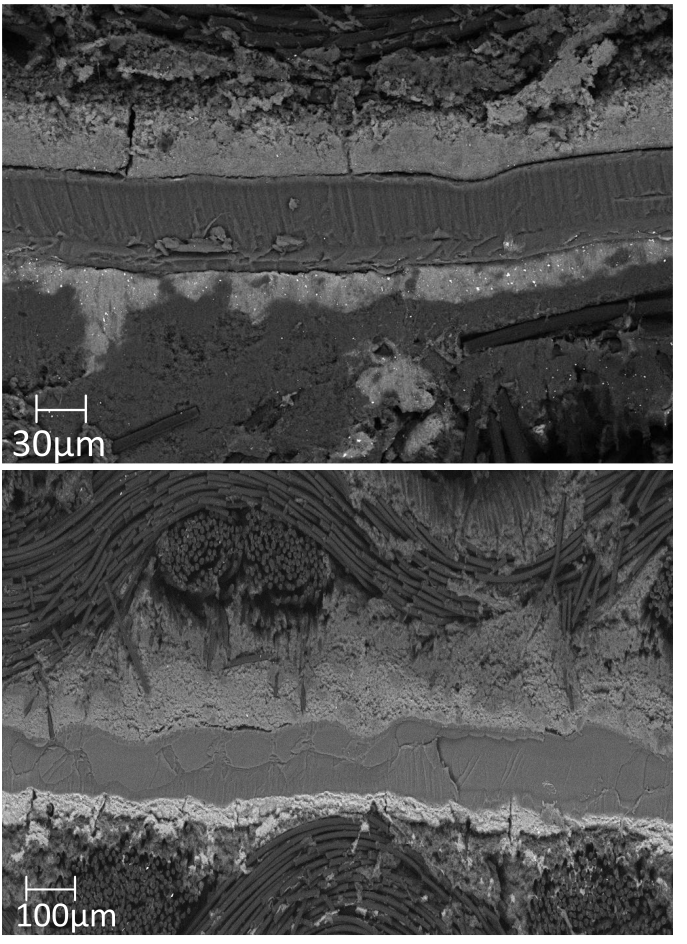

Figure 4.8: Post-mortem analysis of the cross section of a Celtec P- 2100 MEA (a) SEM image of a new MEA and (b) SEM image of a used MEA.

agglomeration. However, the plots represent only one cross-section of each MEA out of many possible cross-sections. Nonetheless, the same trend is seen in other cross-sections as well, indicating that there may be some Pt particle sintering.

Small variations in PA levels in Fig. 4.9 between the new and the used MEA at different points along the cross-section suggest that there is a small PA mobility from the electrolyte to the electrodes. Acid mobility is reported to be quick in the MEA, and can be caused due to compression by the flow plates and by drawing current from the fuel cell [Wannek et al., 2009]. Indeed, PA leaching is suggested to have effects at lower temperatures of fuel cell shut down [Liu et al., 2006]. In this work however, there were no intentional start/stop cycles tested. This may

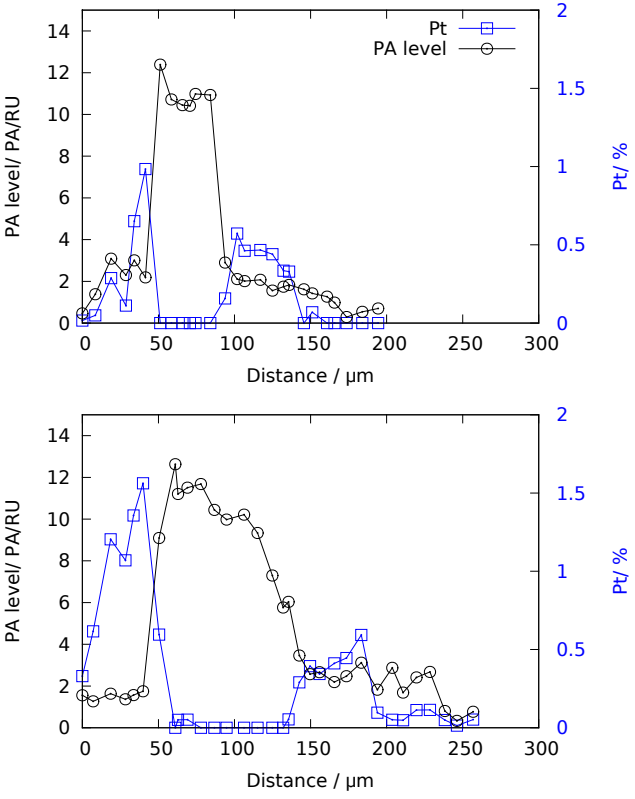

Figure 4.9: Post-mortem analysis of the cross section of a Celtec P- 2100 MEA (a) Pt and PA level distributions of a new MEA and (b) Pt and PA level distributions of a used MEA.

have limited the PA leaching and its effects on the fuel cell.

4.5 Combined Effects of Impurities

The collective effects of impurities on the performance of the fuel cell can be said greater than the arithmetic sum of effects in most cases. This is attributable to the possible reactions among impurities and their intermediates, and catalyst surface adsorptions of complex intermediate formations from the electro-oxidation of methanol on the catalyst surface. In Fig. 4.10, the interdependence among all the reformate impurities are given.

The interaction plots in Fig. 4.10 show some interdependence between the effects of the different impurities. In an interaction plot parallel lines represent that

there is no dependence among effects. Therefore, the less parallel two lines are the more interacting effects they have.

The interaction between the effects of CO and CO_2 seems not to exist for CO concentration below 1%, while on the contrary, a high level of interaction between the effects of the two gases is seen as the CO concentration is raised to 2%. Bhatia and Wang [2004] found that the combined effects of trace quantities of CO and hydrogen dilution have an extremely detrimental effect on the performance of a LT-PEMFC. In this work the interaction is most significant for R_{hf} and R_{if}, Fig. 4.10(b) and (c), and negligible for R_{ohmic}, Fig. 4.10(a). Some interdependence among the effects of these two gases is also seen in [Andreasen et al., 2010].

In LT-PEMFCs the opposite is reported, where the losses due to CO_2 are the largest when the CO content is small [de Bruijn et al., 2002; Yan et al., 2009]. Since the main CO_2 poisoning mechanism in LT-PEMFCs is through CO formation by RWGS, it could be that this effect decreases due to shift in equilibrium direction in the presence of CO. It could also be that, as LT-PEMFCs are very sensitive to CO, the effects of CO_2 are simply too small to be noticed compared to those of CO. However, In HT-PEMFCs the worst effects of CO_2 are observed in the presence of CO [Andreasen et al., 2011], specifically 2% CO in the current work. This is not to say that the effects of CO_2 are worse at higher operating temperatures, but that their interaction with CO are evident at high CO concentrations. The main reason to this kind of interaction might be the same seen in [Bhatia and Wang, 2004], where the combined effects of CO and hydrogen dilution have detrimental effects on the performance of the fuel cell. This could be the result of reduced number of H_2 molecules per active catalyst area.

Slight interdependence among the effects of CO_2 and methanol-water vapor mixture is also seen. The interaction here could be with either methanol itself or with the intermediate formations of its dehydrogenation process, given in Eqn. 4.6. However, the effects of methanol-water vapor mixture do not show interdependence with those of CO, which means their effects are simply additive.

Summary

In summary, the different methanol-based reformate impurities cause performance losses in a fuel cell. This chapter has presented these effects for each reformate constituent, and related such effects to temperature, current density and to each other. The losses are exacerbated when two or more impurities are tested together, due to the interactions that take place among them.

The interaction among effects obtained in this study gives an invaluable first qualitative insight into the tolerable mixes of impurities for optimizing the operating parameters of an HT-PEMFC. This can be an used for tweaking the performance and selectivity of both the fuel cell and the methanol reforming processor in a fuel cell system.

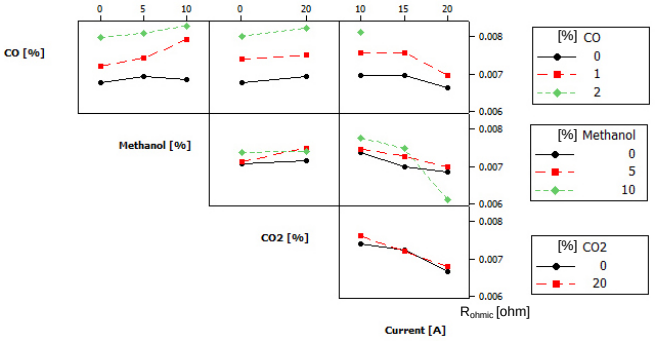

(a)

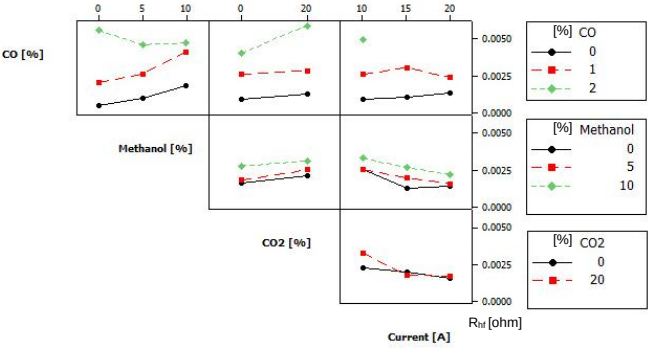

(b)

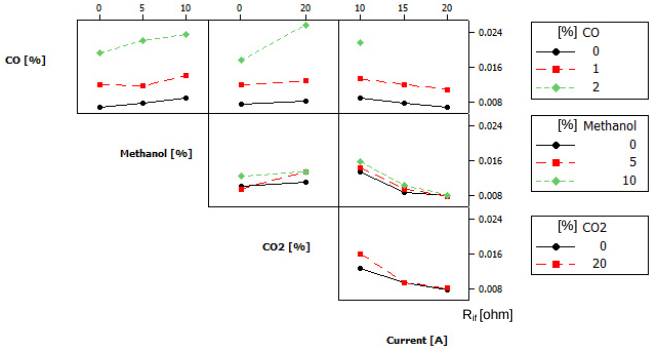

(c)

Figure 4.10: Interaction of effects among the different factors at 160 °C (a) for ohmic resistance (b) high frequency resistance (c) intermediate - low frequency resistance.

5 Conclusion

In this final section a summary of the main conclusions of the current research work is given. The limitations of the work are also given with suggestions for future work to continue the effort to better understand the degradation and lifetime issues of HT-PEMFCs and to improve the test procedures.

5.1 Final remarks

In this dissertation the work of an experimental characterization of a PBI–based HT-PEMFC is reported. The effects of impurities from methanol steam reforming were investigated by means of EIS. To assist in this, a complete unit fuel cell test station was prepared, and a comprehensive testing of all the impurities in a reformate mixture, including methanol and water vapor was done. For a precise, reliable and reproducible delivery of the vapor constituents of the reformate mixture a vapor delivery system, in which a pump was connected to an electrically heated evaporator was developed. The choice of such a system is the result of a study that compared two systems, one based on a bubbler and another based on a pump connected to an evaporator. The latter system was chosen, as it was found to be more suitable for the purposes of the current study.

The fuel cell used in this work is a unit cell assembly of a 45 cm^2 active area with a Celtec® P MEAs from BASF, sandwiched between graphite composite flow plates of serpentine flow channels.

5.1.1 Degradation Due to Non-ideal Conditions

Impedance spectra have been recorded at different operating points, namely different compositions of impurities, and varying temperatures and current densities. The results show that all the impurities present in the reformate gas; CO, CO_2 and methanol-water vapor mixture have poisoning effects on the fuel cell. This is true whether they are introduced individually or collectively as a stream of gases and vapors. Results confirm that the most severe effects are observed in the presence of CO. CO_2 on the other hand has a very minor effects at high operating temperatures, if present alone. High concentrations of methanol-water vapor mixture also have degrading effects and should be considered when optimizing the operating parameters of a reformate gas-fed HT-PEMFC. Other non-ideal conditions, such as decreasing temperature showed similar degrading effects, owing to increased CO–adsorption and decreased electro-oxidation of adsorbed CO.

Factorial analysis showed some of the possible interdependence among the effects of the different impurities. The interaction is most important for CO and CO_2 at CO concentration of 2% by volume, suggesting that tolerance to CO of a PBI-based HT-PEMFC is reduced in the presence of CO_2 in the anode feed gas. The study showed also a small interdependence among the effects of methanol-water vapor mixture and CO_2. Therefore, it can be said that the collective effects of impurities on the performance of the fuel cell are greater than the arithmetic sum of effects in most cases.

Most of the degrading effects caused by the impurities are more pronounced for intermediate-high frequency resistances, implying that charge transfer losses are the most significant losses. This is in agreement with the general literature that most of the poisoning effects are seen at the Pt-catalyst surface, causing loss of ECSA.

5.1.2 Durability in the Presence of Vapor Mixture

Accelerated tests were performed over a period of 1250 hours by changing the methanol-water vapor mixture content of the anode feed. These tests gave a general insight into the effects of the mixture on the performance of the fuel cell. The voltage drop was continuously registered, and EIS measurements were taken and analyzed by fitting to an EC model.

Degradation rate for operation with pure hydrogen was found to be $-5\,\mu$V/h over the first 123 hours after break-in, which is in the same order of magnitude as in the literature. Degradation rates in the presence methanol-water vapor mixture were higher; $-900\,\mu$V/h for 5% and -3.4 mV/h for 8%. Both from durability curve and impedance analysis it is seen that continuous operation with 5% or 8% of vapor mixture degrades the fuel cell severely. Based on literature survey, methanol dehydrogenation on Pt surface with the formation of CO and other complex intermediates, which then poison the catalyst, can be suggested as a degrading mechanism.

Lower concentrations below 3% of vapor mixture, which are more significant

to real world operation, have negligible effect in this work. These lower concentrations were tested after tests at higher concentrations of vapor mixture, and a partial recovery of the cell's performance is seen as a result. This signifies that the effects of the vapor mixture are in part reversible.

Atomic distribution measurements showed a small Pt particle agglomeration and slight PA mobility. However, PA leaching was small and cannot be considered as an issue during continuous operations, where start/stop cycles are not characteristic.

5.2 Future work

As set out in the beginning of this research work, understanding the degrading mechanisms of fuel cells is a good starting point for mitigating them and prolonging the lifetime of fuel cells. This idea has served as the motivation for the work done, and while an insight into the fundamentals of these mechanisms by experimental testing has been provided, further work is needed to better understand and describe them.

In the work reported in *paper 2*, the effect of time in the interdependence among the tested factors is not considered. During testing however, the fuel cell continued to degrade in time, which inevitably changes the starting points for the different measurements at different operating conditions. To avoid this, tests on as many identical unit cell test stations as the number of test points in a controlled environment would be required at very high costs. An easier way of tackling this issue that can be considered for future work can be, including the history effect of time and its interdependence with the other factors, and hence, consider it in the factorial design of experiments. This is recommended for a more complete picture of all the factors affecting the performance of a fuel cell.

EIS as a characterization technique is powerful, and in this work it has been used to perform a variety of tests and to look into the effects of different operating conditions. Nevertheless, its use in conjunction with other electrochemical techniques such as CV, can add more detail to the study. For-example, CV studies of Pt surface coverage by adsorption of impurities (loss of ECSA) can support the changes in the kinetics of the catalyst reactions that are usually manifested by changes in high frequency loops of EIS measurements.

Even though, the effects of vapor mixture have been isolated from those of gaseous species in this dissertation, further isolation of the effects of methanol from those of water vapor can benefit the design of both reformer systems and fuel cells. This could be done with start/stop cycling tests to also reveal whether the vapors could result in PA leaching a lower temperatures.

Lastly, all the tests done in this work were performed on a single cell assembly, and though, operating conditions were varied to simulate real life operations, the presence of other adjacent cells has not been tested. Since fuel cell stacks are used in real life operations, tests need to be extended to this level. Moreover, even though the reformate impurities were simulated in a controlled manner and is

easier to control than a real reforming process, a test station which includes a fuel cell fed from a reformer can give a wider perspective for systems development.

References

Andreasen, S. J., R. Mosbæk, J. R. Vang, S. K. Kær, and S. S. Araya (2010). EIS Characterization of the Poisoning Effects of CO and CO_2 on a PBI Based HT-PEM Fuel Cell. *ASME Conference Proceedings 2010*(44045), 27–36. 52

Andreasen, S. J., J. R. Vang, and S. K. Kær (2011). High temperature PEM fuel cell performance characterisation with CO and CO_2 using electrochemical impedance spectroscopy. *International Journal of Hydrogen Energy 36*(16), 9815–9830. 12, 21, 28, 38, 45, 52

Angela Greiling Keane and Alan Ohnsman (2012). Fuel Cell Frenzy Looks to Convert Obama Favoring Plug-Ins - Businessweek. http://www.businessweek.com/news/2012-06-20/fuel-cell-frenzy-looks-to-convert-obama-favoring-plug-ins. Online; accessed 24-September-2012. 6

Apple Inc. (2012). Apple - Environment - Renewable Energy. http://www.apple.com/environment/renewable-energy/. Online; accessed 12-September-2012. 9

Arsalis, A., M. P. Nielsen, and S. K. Kær (2013). Application of an improved operational strategy on a PBI fuel cell-based residential system for Danish single-family households. *Applied Thermal Engineering 50*(1), 704 – 713. 12

Asghari, S., A. Mokmeli, and M. Samavati (2010). Study of PEM fuel cell performance by electrochemical impedance spectroscopy. *International Journal of Hydrogen Energy 35*(17), 9283–9290. 21

Barsoukov, E. and J. R. Macdonald (2005). *Impedance Spectroscopy: Theory, Experiment, and Applications* (2nd ed.). Wiley - Interscience. 21

Bhatia, K. K. and C.-Y. Wang (2004, June). Transient carbon monoxide poisoning of a polymer electrolyte fuel cell operating on diluted hydrogen feed. *Electrochimica Acta 49*(14), 2333–2341. 52

Bloom, I., L. Walker, J. Basco, T. Malkow, G. De Marco, and G. Tsotridis (2011). A Comparison of Fuel Cell Test Protocols. *ECS Transactions 30*(1), 227–235. 27

Bloom Energy (2012). Customers | Bloom Energy. http://www.bloomenergy.com/customer-fuel-cell/. Online; accessed 12-September-2012. 9

Boer, H. (1995). Mass Flow Controlled Evaporation System. *Journal de Physique IV 05*(5), 961–966. 29

Borup, R., J. Meyers, B. Pivovar, Y. S. Kim, R. Mukundan, N. Garland, D. Myers, M. Wilson, F. Garzon, D. Wood, P. Zelenay, K. More, K. Stroh, T. Zawodzinski, J. Boncella, J. E. McGrath, M. Inaba, K. Miyatake, M. Hori, K. Ota, Z. Ogumi, S. Miyata, A. Nishikata, Z. Siroma, Y. Uchimoto, K. Yasuda, K.-I. Kimijima, and N. Iwashita (2007, October). Scientific aspects of polymer electrolyte fuel cell durability and degradation. *Chemical reviews 107*(10), 3904–51. 19, 38

Breakthrough Technologies Institute Inc. (2012). 2011 Fuel cell Technologies Market Report. Technical Report July. xv, 6, 7, 8

Bromberg, L. and W. K. Cheng (2010). Methanol as an Alternative Transportation Fuel in the U.S.: Options for Sustainable and/or Energy-Secure Transportation. Technical report, Massachusetts Institute of Technology, Sloan Laboratories for Automotive and Aircraft Engines Cambridge, MA 02139 USA Battelle Columbus, OH USA. 16

Büchi, F. N., M. Inaba, and T. J. Schmidt (2009). *Polymer Electrolyte Fuel Cell Durability*. Springer New York. 28, 38

Calundann, G. (2006). High Temperature PEM Fuel Cells: The New Generation. Technical report. 15

Cao, D., G.-Q. Lu, A. Wieckowski, S. A. Wasileski, and M. Neurock (2005, June). Mechanisms of methanol decomposition on platinum: A combined experimental and ab initio approach. *The journal of physical chemistry. B 109*(23), 11622–33. 20, 43

Carter, D. (2012). Fuel Cell Residential Micro-CHP Developments in Japan. Technical Report February. 8

Cheng, X., Z. Shi, N. Glass, L. Zhang, J. Zhang, D. Song, Z.-S. Liu, H. Wang, and J. Shen (2007). A review of PEM hydrogen fuel cell contamination: Impacts, mechanisms, and mitigation. *Journal of Power Sources 165*(2), 739 – 756. 23, 40

Daletou, M. K., J. K. Kallitsis, G. Voyiatzis, and S. G. Neophytides (2009). The Interaction of Water Vapors with H_3PO_4 Imbibed Electrolyte Based on PBI/polysulfone Copolymer Blends. *Journal of Membrane Science 326*(1), 76–83. 46, 47

Danish Energy Agency (2009, March). Danish Climate and Energy Policy. `http://www.ens.dk/en-US/policy/danish-climate-and-energy-policy/Sider/danish-climate-and-energy-policy.aspx`. Online; accessed 27-August-2012. 2

Danish Partnership for Hydrogen and Fuel Cell (2012). Danish success stories – why Danish fuel cells will be a success. http://www.hydrogennet.dk/384/. Online; accessed 16-October-2012. 12

Das, S. K., A. Reis, and K. J. Berry (2009). Experimental evaluation of CO poisoning on the performance of a high temperature proton exchange membrane fuel cell. *Journal of Power Sources 193*(2), 691–698. 28, 38

de Bruijn, F., V. A. T. Dam, and G. J. M. Janssen (2008, February). Review: Durability and Degradation Issues of PEM Fuel Cell Components. *Fuel Cells 8*(1), 3–22. 21, 24, 38

de Bruijn, F., D. Papageorgopoulos, E. Sitters, and G. Janssen (2002). The influence of carbon dioxide on PEM fuel cell anodes. *Journal of Power Sources 110*(1), 117 – 124. 42, 52

DOE (2007, March). DOE Cell Component Accelerated Stress Test Protocols for PEM Fuel Cells. 27

Du, B., R. Pollard, J. F. Elter, and M. Ramani (2009). Performance and Durability of a Polymer Electrolyte Fuel Cell Operating with Reformate: Effects of CO, CO_2, and Other Trace Impurities. In F. N. Büchi, M. Inaba, and T. J. Schmidt (Eds.), *Polymer Electrolyte Fuel Cell Durability*, pp. 341–366. 16, 19, 38, 41

Fouquet, N., C. Doulet, C. Nouillant, G. Dauphin-Tanguy, and B. Ould-Bouamama (2006). Model based PEM fuel cell state-of-health monitoring via ac impedance measurements. *Journal of Power Sources 159*(2), 905–913. 21

Fuel Cell Today (2011). The Fuel Cell Today Industry Review 2011. Technical report, Fuel Cell Today. xv, 5, 6, 11

Fuel Cell Today (2012). The Fuel Cell Today Industry Review 2012. Technical report. 6

Gomadam, P. M. and J. W. Weidner (2005, October). Analysis of electrochemical impedance spectroscopy in proton exchange membrane fuel cells. *International Journal of Energy Research 29*(12), 1133–1151. 49

Gu, T., S. Shimpalee, J. Van Zee, C.-Y. Chen, and C.-W. Lin (2010, December). A study of water adsorption and desorption by a PBI-H_3PO_4 membrane electrode assembly. *Journal of Power Sources 195*(24), 8194–8197. 46

Guilminot, E., A. Corcella, M. Chatenet, F. Maillard, F. Charlot, G. Berthomé, C. Iojoiu, J.-Y. Sanchez, E. Rossinot, and E. Claude (2007). Membrane and Active Layer Degradation upon PEMFC Steady-State Operation. *Journal of The Electrochemical Society 154*(11), B1106. 21, 24

Higier, A. and H. Liu (2012). Separate in situ measurements of ECA under land and channel in PEM fuel cells. *Journal of Power Sources 215*(0), 11 – 17. 23

Honnery, D. and P. Moriarty (2009). Estimating global hydrogen production from wind. *International Journal of Hydrogen Energy 34*(2), 727 – 736. 16

Hu, J., H. Zhang, Y. Zhai, G. Liu, J. Hu, and B. Yi (2006). Performance degradation studies on PBI/H_3PO_4 high temperature PEMFC and one-dimensional numerical analysis. *Electrochimica Acta 52*(2), 394 – 401. 24

Hu, J., H. Zhang, Y. Zhai, G. Liu, and B. Yi (2006). 500 h Continuous aging life test on PBI/H_3PO_4 high-temperature PEMFC. *International Journal of Hydrogen Energy 31*(13), 1855 – 1862. 24

Hydrogen Link Denmark Association (2012, March). Danish Government to launch hydrogen Infrastructure Program & continue FCEV tax exemptions throughout 2015. http://www.hydrogenlink.net/eng/PR-Danish-Government-launch-hydrogen-initiatives-23-03-2012.asp. Online; accessed 16-October-2012. 12

IEA (2007). IEA Energy Technology Essentials - Hydrogen Production and Distribution. Technical report, International Energy Agency (IEA). 16

IEA (2012). IEA - May: Global carbon - dioxide emissions increase by 1.0 Gt in 2011 to record high. Technical report. 1

International Labour Organization (2012). *Working towards sustainable development: Opportunities for decent work and social inclusion in a green economy*. International Labour Office. 3

Iojoiu, C., E. Guilminot, F. Maillard, M. Chatenet, J.-Y. Sanchez, E. Claude, and E. Rossinot (2007). Membrane and Active Layer Degradation Following PEMFC Steady-State Operation. *Journal of The Electrochemical Society 154*(11), B1115–B1120. 21, 24

Iwasita, T. (2002, August). Electrocatalysis of methanol oxidation. *Electrochimica Acta 47*(22-23), 3663–3674. 20, 43

Jesper Lebæk (2010). *Experimental Characterization and Modeling of PEM Fuel Cells*. Ph. D. thesis. xiii, 23

Ji, X., L. Yan, S. Zhu, L. Zhang, and W. Lu (2008). Methanol Distribution and Electroosmotic Drag in Hydrated Poly (perfluorosulfonic) Acid Membrane. *The Journal of Physical Chemistry B 112*(49), 15616–15627. 47

Jian, X., V. W. J. Kennard, and Z. Thomas (2002, January). Porosimetric study of catalyst layer of polymer electrolyte fuel cell (PEFC). In *Conference: Submitted to 202nd Meeting of the Electrochemical Society, Salt Lake City, UT, Oct. 2002*. Los Alamos National Laboratory. 21

Jiang, R., H. R. Kunz, and J. M. Fenton (2005). Electrochemical Oxidation of H_2 and H_2/CO Mixtures in Higher Temperature (T_{Cell} > 100 °C) Proton Exchange Membrane Fuel Cells: Electrochemical Impedance Spectroscopy. *Journal of The Electrochemical Society 152*(7), A1329–A1340. 39

JRC-IE (2010, April). PEFC power stack performance testing procedure Measuring voltage and power as function of time and current density Long term durability steady test. 27

Kongstein, O., T. Berning, B. Børresen, F. Seland, and R. Tunold (2007). Polymer electrolyte fuel cells based on phosphoric acid doped polybenzimidazole (PBI) membranes. *Energy 32*(4), 418 – 422. 24

Kundu, S., M. Fowler, L. C. Simon, and R. Abouatallah (2008). Reversible and irreversible degradation in fuel cells during Open Circuit Voltage durability testing. *Journal of Power Sources 182*(1), 254 – 258. 38

Li, Q., R. He, J.-A. Gao, J. O. Jensen, and N. J. Bjerrum (2003). The CO Poisoning Effect in PEMFCs Operational at Temperatures up to 200 °C. *Journal of The Electrochemical Society 150*(12), A1599. 16, 19, 23, 38, 39

Li, Q., R. He, J. Jensen, and N. Bjerrum (2004, August). PBI–Based Polymer Membranes for High Temperature Fuel Cells -Preparation, Characterization and Fuel Cell Demonstration. *Fuel Cells 4*(3), 147–159. 14

Li, Q., J. O. Jensen, R. F. Savinell, and N. J. Bjerrum (2009). High Temperature Proton Exchange Membranes Based on Polybenzimidazoles for Fuel Cells. *Progress in Polymer Science 34*(5), 449–477. 12, 14, 16, 19, 44

Liu, G., H. Zhang, J. Hu, Y. Zhai, D. Xu, and Z.-g. Shao (2006, November). Studies of performance degradation of a high temperature PEMFC based on H_3PO_4–doped PBI. *Journal of Power Sources 162*(1), 547–552. 19, 23, 24, 46, 47, 49, 50

Lobato, J., P. Cañizares, M. A. Rodrigo, and J. J. Linares (2007). PBI-based polymer electrolyte membranes fuel cells: Temperature effects on cell performance and catalyst stability. *Electrochimica Acta 52*(12), 3910 – 3920. 24

Lohr, S. (2012). The Patent Clues to the Apple iPhone Beyond '5' - NYTimes.com. http://bits.blogs.nytimes.com/2012/09/12/the-patent-clues-to-the-apple-iphone-beyond-5/. Online; accessed 12-September-2012. 9

Love, A., S. Middleman, and A. K. Hochberg (1993). The Dynamics of Bubblers as Vapor Delivery Systems. *Journal of Crystal Growth 129*(1-2), 119–133. 30

Lynch, B., P. L. Narasimham, and F. P. Partus (1986). Methods of and apparatus for vapor delivery control in optical preform manufacture. U.S. Patent 4582480. 29

Mamlouk, M. and K. Scott (2011). Analysis of high temperature polymer electrolyte membrane fuel cell electrodes using electrochemical impedance spectroscopy. *Electrochimica Acta 56*(16), 5493–5512. 21, 45, 46

marketsandmarkets.com (2011, Dicember). Hydrogen Generation Market - by Merchant & Captive Type, Distributed & Centralized Generation, Application & Technology - Trends & Global Forecasts (2011 - 2016). Technical report, marketsandmarkets.com. 16

Martin, S. and A. Wörner (2011). On-board reforming of biodiesel and bioethanol for high temperature PEM fuel cells: Comparison of autothermal reforming and steam reforming. *Journal of Power Sources 196*(6), 3163 – 3171. 12

McConnell, V. P. (2009, December). High-temperature PEM fuel cells: Hotter, simpler, cheaper. *Fuel Cells Bulletin 2009*(12), 12–16. 12

Mcmenamin, J. C. (1983). Vapor Mass Flow Control System. U.S. Patent 4393013. 29

Mcmenamin, J. C. (1984). Vapor Mass Flow Control System. U.S. Patent 4436674. 29

Moçotéguy, P., B. Ludwig, J. Scholta, R. Barrera, and S. Ginocchio (2009, August). Long Term Testing in Continuous Mode of HT-PEMFC Based H_3PO_4/PBI Celtec-P MEAs for μ-CHP Applications. *Fuel Cells 9*(4), 325–348. 44, 46, 47

Modestov, A., M. Tarasevich, and H. Pu (2012). Investigation of methanol electrooxidation on Pt and Pt–Ru in H_3PO_4 using MEA with PBI–H_3PO_4 membrane. *Journal of Power Sources 205*(0), 207 – 214. 20, 43

Monk, P. (2007). *Fundamentals of Electroanalytical Chemistry*. Analytical Techniques in the Sciences. John Wiley & Sons, Ltd. 22

Olah, G. A., A. Goeppert, and G. K. S. Prakash (2009). *Beyond Oil and Gas: The Methanol Economy*. Wiley. 16

Oliver, J., G. Janssens-Maenhout, and J. Peters (2012). Trends in global CO_2 emissions; 2012 Report. Technical report, PBL Netherlands Environmental Assessment Agency. xiii, 2

Orazem, M. E. and B. Tribollet (2008). *Electrochemical Impedance Spectroscopy*. John Wiley & Sons, Inc. 21

Otomo, J., X. Li, T. Kobayashi, C.-j. Wen, H. Nagamoto, and H. Takahashi (2004, November). AC-impedance spectroscopy of anodic reactions with adsorbed intermediates: electro-oxidations of 2-propanol and methanol on carbon-supported Pt catalyst. *Journal of Electroanalytical Chemistry 573*(1), 99–109. 46

Partus, F. P. (1980). Vapor Delivery System and Method. U.S. Patent 4220460. 29

Pattamarat, K. and M. Hunsom (2008). Testing of PEM fuel cell performance by electrochemical impedance spectroscopy: Optimum condition for low relative humidification cathode. *Korean Journal of Chemical Engineering 25*(2), 245–252. 21

Qi, Z. and S. Buelte (2006). Effect of open circuit voltage on performance and degradation of high temperature PBI–H_3PO_4 fuel cells. *Journal of Power Sources 161*(2), 1126 – 1132. 24

REN21 (2012). Renewables 2012 Global Status Report. Technical report, REN21, Renewable Energy Policy Network for the 21st Century. 1, 2

Ross, E. A. (1977). Saturated liquid/vapor generating and dispensing. U.S. Patent 4051886. 29

Ryan O'Hayre (2004). *Micro Scale Electrochemistry: Application to Fuel Cells*. Phd thesis, Stanford University. 3, 20

Savinell, R. F. and M. H. Litt (1998). Proton conducting polymers prepared by direct acid casting. U.S. Patent 5716727. 14

Schipper, L., H. Fabian, and J. Leather (2009). ADB Sustainable Development Working Paper Series Transport and Carbon Dioxide Emissions : Forecasts , Options Analysis , and Evaluation Transport and Carbon Dioxide Emissions : Forecasts , Options Analysis , and Evaluation. *Asian Development Bank* (9). 6

Schmidt, T. J. (2006, June). Durability and Degradation in High-Temperature Polymer Electrolyte Fuel Cells. In *ECS Transactions*, Volume 1, pp. 19–31. ECS. 18, 20, 23

Schmidt, T. J. and J. Baurmeister (2008, February). Properties of high-temperature PEFC Celtec®-P 1000 MEAs in start/stop operation mode. *Journal of Power Sources 176*(2), 428–434. 19, 20, 43

Seland, F., T. Berning, B. Børresen, and R. Tunold (2006). Improving the performance of high-temperature PEM fuel cells based on PBI electrolyte. *Journal of Power Sources 160*(1), 27 – 36. 24

Sethuraman, V. A., B. Lakshmanan, and J. W. Weidner (2009). Quantifying desorption and rearrangement rates of carbon monoxide on a PEM fuel cell electrode. *Electrochimica Acta 54*(23), 5492 – 5499. 23

Silva, E. D., A. M. Neto, P. Ferreira, J. Camargo, F. Apolinàrio, and C. Pinto (2005). Analysis of hydrogen production from combined photovoltaics, wind energy and secondary hydroelectricity supply in Brazil. *Solar Energy 78*(5), 670 – 677. 16

Smithsonian Institution (2004). Collecting the History of Proton Exchange Membrane Fuel Cells. `http://americanhistory.si.edu/fuelcells/pem/pemmain.htm`. Online; accessed 13-September-2012. 4

Song, C., S. R. Hui, and J. Zhang (2008). High-temperature PEM Fuel Cell Catalysts and Catalyst Layers. pp. 861–888. Springer London. 19, 20, 38, 39

Spare; Bradley L. ; et al. (2010). Fuel Cell System To Power A Portable Computing Device. United States Patent Application 20110311895. 9

Sriramulu, S., T. Jarvi, and E. Stuve (1999). Reaction mechanism and dynamics of methanol electrooxidation on platinum(111). *Journal of Electroanalytical Chemistry 467*(1-2), 132 – 142. 43

University of Cambridge (2012). Electrochemistry Group Fuel Cell. http://www.cheng.cam.ac.uk/research/groups/electrochem/JAVA/electrochemistry/ELEC/l10html/main.html. Online; accessed 13-September-2012. 4

U.S. Department of Energy (2012). Fuel Cell Technologies Program: Fuel Cell Technologies Program Multi-Year Research, Development and Demonstration Plan. 7

U.S. Department of Energy, DOE (2011). Fuel Cell Technology Challenges. http://www1.eere.energy.gov/hydrogenandfuelcells/fuelcells/fc_challenges.html. Online; accessed 16-October-2012. 7, 17

USFCC (2006, July). USFCC Single Cell Test Protocol. 27

Volvo (2004, June). Specification of Test Procedures for Polymer Electrolyte Fuel Cell Stacks. 27

W. Crabtree, G., M. S. Dresselhaus, and M. V. Buchanan (2004, December). The hydrogen economy. *Physics Today*, 39. 16

Wainright, J., J. Wang, D. Weng, R. Savinell, and M. Litt (1995). Acid–Doped Polybenzimidazoles: A New Polymer Electrolyte. *Journal of the Electrochemical Society 142*(7), L121–L123. 14

Wang, J., R. Savinell, J. Wainright, M. Litt, and H. Yu (1996). A H_2/O_2 fuel cell using acid doped polybenzimidazole as polymer electrolyte. *Electrochimica Acta 41*(2), 193 – 197. 12

Wannek, C., I. Konradi, J. Mergel, and W. Lehnert (2009). Redistribution of phosphoric acid in membrane electrode assemblies for high-temperature polymer electrolyte fuel cells. *International Journal of Hydrogen Energy 34*(23), 9479 – 9485. 50

Wu, J., X. Yuan, J. Martin, and H. Wang (2008). A review of PEM fuel cell durability: Degradation mechanisms and mitigation strategies. *Journal of Power Sources 184*, 104–119. 15, 17

Wu, J., X. Z. Yuan, H. Wang, M. Blanco, J. J. Martin, and J. Zhang (2008). Diagnostic tools in PEM fuel cell research: Part I Electrochemical techniques. *International Journal of Hydrogen Energy 33*(6), 1735 – 1746. 23

Yan, W.-M., H.-S. Chu, M.-X. Lu, F.-B. Weng, G.-B. Jung, and C.-Y. Lee (2009). Degradation of proton exchange membrane fuel cells due to CO and CO_2 poisoning. *Journal of Power Sources 188*(1), 141–147. 28, 38, 52

Yu, S., L. Xiao, and B. C. Benicewicz (2008). Durability Studies of PBI–based High Temperature PEMFCs. *Fuel Cells 8*(3-4), 165–174. 19

Yuan, X., H. Wang, J. C. Sun, and J. Zhang (2007). AC impedance technique in PEM fuel cell diagnosis–A review. *International Journal of Hydrogen Energy 32*(17), 4365–4380. 22

Yuan, X.-Z., C. Song, H. Wang, and J. Zhang (2010). *Electrochemical Impedance Spectroscopy in PEM Fuel Cells: Fundamentals and Applications*. Springer. 21

Zhang, J., Y. Tang, C. Song, and J. Zhang (2007). Polybenzimidazole–membrane–based PEM fuel cell in the temperature range of 120-200 °C. *Journal of Power Sources 172*(1), 163 – 171. 24

Zhang, J., Z. Xie, J. Zhang, Y. Tang, C. Song, T. Navessin, Z. Shi, D. Song, H. Wang, D. P. Wilkinson, Z.-S. Liu, and S. Holdcroft (2006). High temperature PEM fuel cells. In *Journal of Power Sources*, Volume 160, pp. 872–891. 19, 28, 38

Zhang, J., L. Zhang, C. Bezerra, H. Li, Z. Xia, A. Marques, and E. Marques (2009, February). EIS-assisted performance analysis of non-noble metal electrocatalyst (Fe-N/C)-based PEM fuel cells in the temperature range of 23 - 80 °C. *Electrochimica Acta 54*(6), 1737–1743. 19, 21, 48